USRL Research Report No. 71
26 June 1964

PRACTICAL ASPECTS OF PULSED SOUND MEASUREMENTS

C. L. Darner

Department of the Navy — Office of Naval Research
UNDERWATER SOUND REFERENCE LABORATORY
P. O. Box 8337 — Orlando, Florida

DISCLAIMER NOTICE

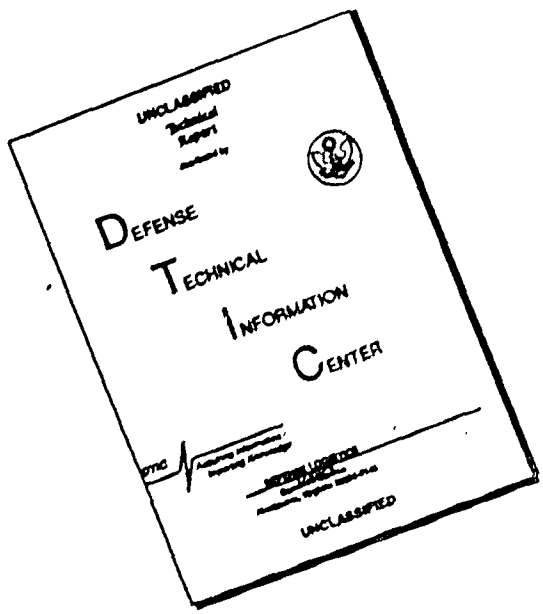

THIS DOCUMENT IS BEST QUALITY AVAILABLE. THE COPY FURNISHED TO DTIC CONTAINED A SIGNIFICANT NUMBER OF PAGES WHICH DO NOT REPRODUCE LEGIBLY.

ABSTRACT

The composition of pulses and their use in underwater sound measurements are examined from a nonclassical viewpoint. The multiple aspects of the complicated subject of pulse modulation are treated with particular consideration for the practitioner rather than the mathematician or the theoretical physicist.

Exception is taken to the following generally held notions concerning pulsed measurements: 1. If the response of the device being measured is to approach the steady-state condition, the number of cycles in the driving pulse must equal the Q of the driven device at the operating frequency. 2. The buildup and decay times of the pulse are equal. 3. The frequency of the received signal is the same as that of the transmitted signal.

FOREWORD

The material in this report was originally compiled as working notes for employees at this laboratory, and was not intended for further distribution. Because of widespread interest in the subject, however, and numerous requests for the material in its present form, it is now being published as a USRL Research Report without extensive revision. It is hoped that the information will be useful in this form.

BLANK PAGE

CONTENTS

ILLUSTRATIONS

Fig.

BLANK PAGE

PRACTICAL ASPECTS OF PULSED SOUND MEASUREMENTS

INTRODUCTION

Pulsed sound techniques have been used for calibrating and testing underwater sound transducers and materials for about 20 years. Patent No. 2,451,509, "Testing Devices for Sound Projectors," was issued to O. M. Owsley in 1948 for this evaluation method. The technique is used when interference from boundaries makes c-w methods impracticable. Boundary interference is eliminated by connecting the hydrophone (or "gating" it) only while the pulse arriving by the straight-line path is impinging on the hydrophone. At all other times, when interfering pulses are arriving, the hydrophone measuring circuit is inoperative.

The chief disadvantage of the pulsing technique is that a pulse consists of a spectrum of frequencies, whereas a c-w signal may contain only one frequency. It is the effect of the filter bandwidth, the pulse length, and the pulse repetition rate on this spectrum that causes most of the problems in pulse measurements.

If all the equipment and conditions for pulsed measurements satisfied the ideal conditions, there would be little reason for this report. If "ideal conditions" existed, the pulse would contain the number of cycles required to approximate a steady-state or c-w condition in the device being measured. All transducers and measuring systems would, under ideal conditions, possess flat frequency response characteristics so that pulse buildup would be instantaneous upon initiation and the decay would be complete and immediate upon termination of the excitation. The satisfaction of these improbable conditions would place the pulsing technique on an elementary level equivalent to making c-w measurements in a large body of water.

Violation of these ideal conditions is always to be expected, however, when measurements are made in a bounded region where sidewall reflections or unwanted diffraction from reflecting plates restricts the pulse length to a small number of cycles at low frequencies. This paucity of cycles always causes considerable doubt as to whether an approximate c-w state has been established. Suspicions about inaccuracy of test data may be allayed by a study of the pulse composition and an understanding of the theoretical limitations imposed by the pulse method of measurement. It is the purpose of this report to present such a study.

Much excellent material has been published during recent years on the analysis of circuit transients. In fact, one 300-page text on pulses gives 200 references to other textbooks and published technical papers. Many articles have been written concerning television and radar systems, but

the use of pulsed wave trains to test sonar devices is mentioned only occasionally, although this use has become widespread.

To cover the entire theory of pulse modulation in a research report is not only infeasible, but impossible. In fact, it might be more helpful to omit the theory and to discuss only its application to specific underwater sound problems. A cursory discussion of pulses is presented, however, as a review for those already familiar with the subject and as an introduction for others.

The transient or pulsed behavior of networks can be analyzed by a number of methods. Some of them are:

1. Differential equations (classical method)
2. Heaviside operational calculus
3. Fourier and Laplace transforms
4. Fourier integral

The Fourier integral method was chosen for discussion here, not only for its relative simplicity, but also because electric waveforms rather than analytical functions can be dealt with. This method gives the engineer an immediate mental picture from which an approximate graphical solution can be obtained without laborious calculation.

THEORY

In 1822 Fourier stated his important mathematical theorem which, for our present purpose, may be expressed as follows: "Any continuous single-valued periodic function can be expressed as a summation of simple harmonic terms having frequencies that are multiples of that of the given function." The series that results from Fourier's theorem may be expressed:

$$x = A_0 + A_1 \cos \omega t + A_2 \cos 2\omega t + \ldots + A_r \cos r\omega t \ldots + B_1 \sin \omega t + B_2 \sin 2\omega t + \ldots + B_r \sin r\omega t \ldots \quad (1)$$

where x is the instantaneous value of the function at time t; the coefficients A_1, A_2, B_1, etc., are the arbitrary maximal amplitudes of the terms; and $\omega = 2\pi f$, where f is the fundamental frequency of the function.

As an illustration, Fig. 1a represents the waveform produced by a woman's voice pronouncing the vowel "i." A Fourier analysis of the wave, depicted in Fig. 1b, shows the amplitude of the fundamental compared with that of fourteen harmonic frequencies. There are probably many higher harmonics that are not shown in this figure.

The pulse modulating envelopes that occur in underwater sound testing lie between the limits of square and triangular waves. Triangular wave modulation is closely approximated by the cosine-squared waveform shown in Fig. 2 together with the square and half-cosine wave shapes. The reason for choosing these three forms will be brought out in the section "Essential Bandwidth."

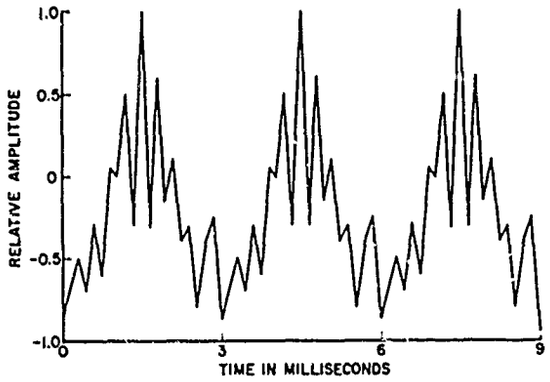

Fig. 1a. Complex waveform produced by voice.

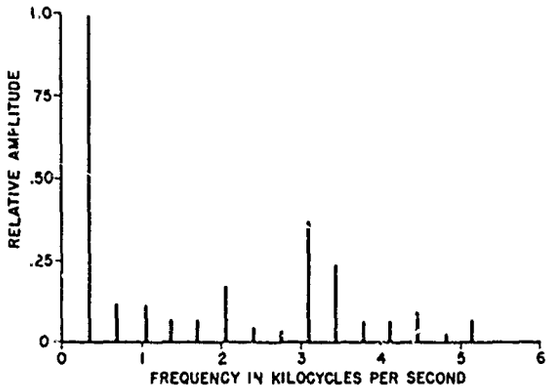

Fig. 1b. Fourier analysis of voice waveform.

The authors of various texts on pulses use two methods of presentation. In Fig. 2, zero time is shown at the center of the pulse. This method is used with the concept of negative frequencies, which will be discussed later. The figure could have been plotted with zero time at the start of the pulse, thus changing the curves from cosine to sine functions. The choice of presentation is largely arbitrary, but there is some preference for starting the pulse at zero time. In this report, emphasis will be placed on discussion of the square or rectangular pulse, with only occasional reference to the other two types. It is well, however, to recognize the existence of the other modulation envelopes because of their frequent occurrence. When short sequential pulses are started at different points on a sinusoidal wave, the modulation envelope will vary from pulse to pulse.

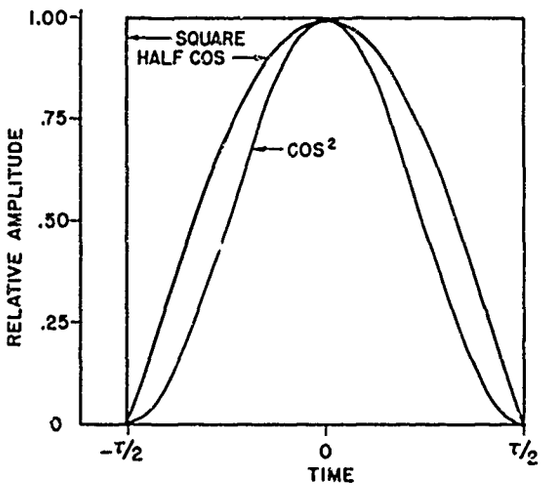

Fig. 2. Comparison of three pulse envelope shapes.

Evaluation of the constants in Eq. 1 gives the analytical form for a square wave with zero amplitude occurring at zero time as shown in Fig. 3a:

$$x = (4a/\pi)[\sin \omega t + (1/3)\sin 3\omega t + (1/5)\sin 5\omega t + \ldots] \qquad (2)$$

For zero time occurring at the midpoint of the maximum of the square wave as shown in Fig. 2, the analytical form would be:

$$x = (4a/\pi)[\cos \omega t - (1/3)\cos 3\omega t + (1/5)\cos 5\omega t - \ldots] \qquad (2a)$$

The two formulae give equivalent results.

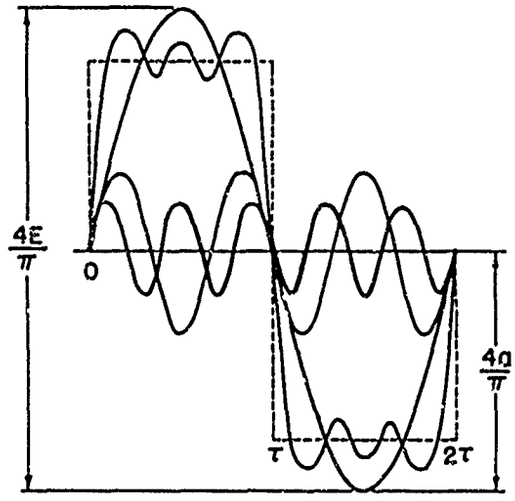

Fig. 3a. Approximation to a square wave by combination of the primary frequency and two harmonics.

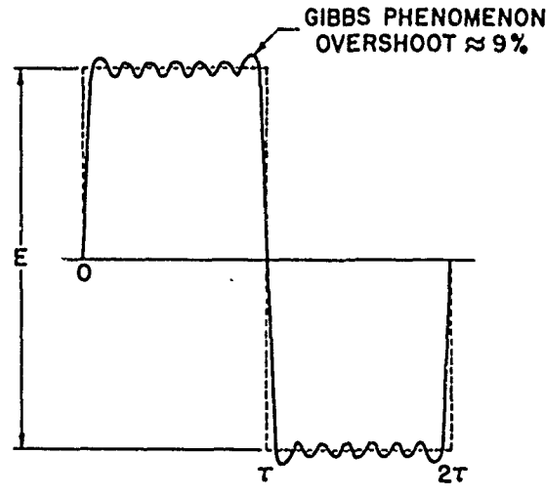

Fig. 3b. Twelve more harmonics added to Fig. 3a.

Only the fundamental and the first two odd harmonic terms are plotted in Fig. 3a, but the resemblance of their sum to a square wave is readily seen. Some residual ripple still exists even after the first fifteen odd terms are summed as in Fig. 3b, but as still higher harmonics are added, the synthetic curve approaches a square wave except at the points of discontinuity. At these points, little "towers" appear. The formation of these towers is called Gibb's phenomenon in the Fourier series. For a function whose period is 2π, the amplitude of these irregularities is, in general, 0.0895 of the square wave amplitude. According to Goldman [1], "These towers are actually equal to the negative of the sum of the terms beyond the last term used in making the graph of the function from its Fourier series. As the number of terms used is increased, the total area of the tower decreases; but, instead of decreasing in height, the tower becomes narrower. However, this is not surprising, for as the limiting process progresses, the tower represents higher and higher frequency terms. The limiting process of summing the Fourier series thus has no necessary effect on the height of the tower, even though it continually decreases its area."

The first term A_0 in the expression for a Fourier series (Eq. 1) is a constant that can represent a d-c component that, when added to the series, displaces the square wave upward so that the bottom of the square wave coincides with the base line. The square wave then becomes a square pulse for modulation purposes.

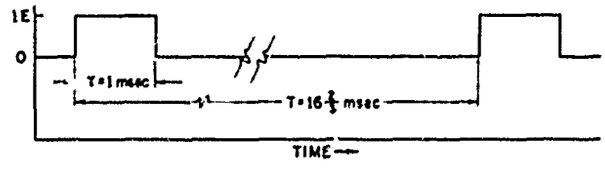

Fig. 4a. Square pulses at the repetition rate 60 pps.

Typical pulse shapes used at the USRL are shown in Fig. 4a. The repetition rate is ordinarily the power line frequency (60 cps) or, occasionally, some multiple or submultiple thereof. The proximity of reflecting

boundaries usually limits the length of the pulse for transducer tests to approximately 1 msec. The primary frequency of the spectrum of this 1-msec pulse is 500 cps, comprising only the first half-cycle of the square wave shown in Fig. 3. In this report, the frequency is described as "primary" only when explicit reference is made to the lowest frequency contained in the spectrum of the square pulse.

The duty cycle K is the ratio of the pulse length τ and the time interval T between initiation of successive pulses, which is the reciprocal of the repetition rate. (Note: K is arbitrarily defined in some texts as the inverse of this ratio.) For Fig. 4a,

$$K = \tau/T = 0.001/0.0167 = 0.06 = 6\%.$$

When K is considerably less than one, the relative amplitude A_n/K of any spectral frequency (n) can be calculated by the following formula from Terman [2],

$$A_n/K = [2E \sin(nK\pi)]/(nK\pi), \qquad n = 1, 2, 3, \ldots \qquad (3)$$

where E is the amplitude of the square wave. The absolute amplitudes of these frequencies are obtained by multiplying the relative amplitudes by K.

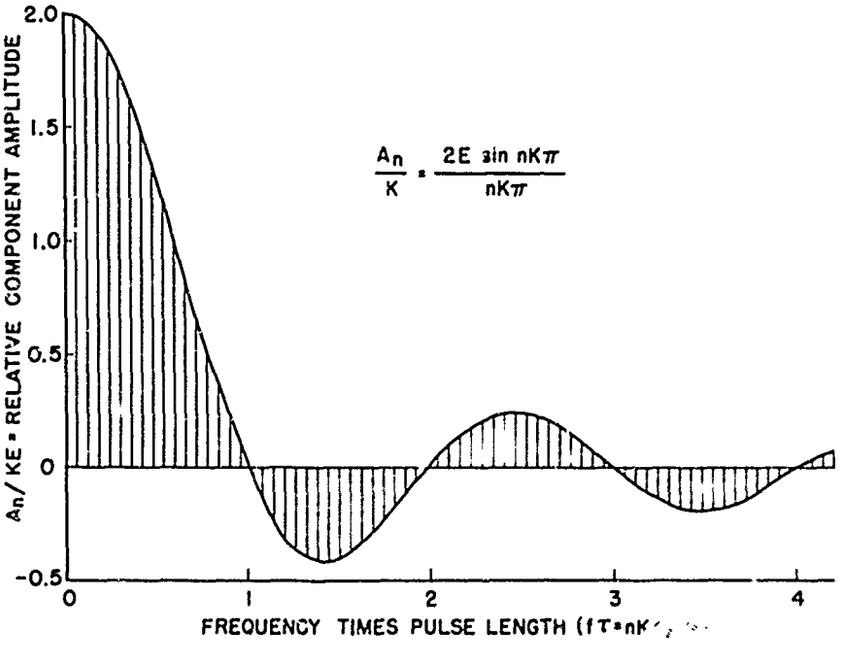

Fig. 4b. Normalized plot of the Fourier spectrum for square pulses. For pulses of Fig. 4a, the spacing of the vertical frequency lines represents 60 cps.

Figure 4b can be used to analyze a square pulse of any length. The units of the abscissa are cycles. When these units are divided by the pulse length of the square wave under analysis, the abscissa then represents the spectral frequencies making up the square pulse. The relative amplitudes of these frequencies in terms of the height E of the square pulse are given by the ordinates. The plotting of spectral lines below

the abscissa indicates reversal of phase. This phase reversal also was shown in Fig. 3a midway between 0 and τ. When the primary frequency of Fig. 3a is at its peak, the 3rd harmonic maximum is 180° out of phase and the 5th harmonic maximum is again in phase, in conformity with Eq. 2a.

In the example for a 1-msec pulse, the unit cycle of Fig. 4b becomes 1/0.001 = 1 kc; the vertical lines are then arbitrarily spaced at 0.06/0.001 = 60 cps, the repetition rate for this example. If the pulse length were increased tenfold, the first intersection of the curve with the abscissa would represent 100 cps, and a much narrower band of frequencies would contain most of the pulse.

The maxima of the lobes appearing at 1.5, 2.5, 3.5, etc., are the relative levels of the third, fifth, and seventh harmonics, respectively, that make up the square pulse shown in Fig. 3a. Notice the absence of spectral frequencies at points on the abscissa labeled 1, 2, 3, etc., representing, for a 1-msec pulse, integral multiples of 1 kc. These are the even harmonics of the 500-cps primary frequency, and also are shown by Eq. (2) to be absent from a square pulse.

The maximal amplitude of each harmonic is its numerical reciprocal multiplied by the amplitude of the primary frequency. The amplitudes of the harmonics are important when steep response slopes, such as occur in the characteristics of typical electroacoustic projectors, cause asymmetric amplification of the sidebands. More explanation may be worthwhile.

The primary frequency of the 1-msec pulse is 500 cps and lies, therefore, midway between 0 and 1 kc in Fig. 4b. Its amplitude relative to that of the square wave is $4E/\pi$ or 1.27E as was shown in Fig. 3a. The amplitudes of the 3rd, 5th, 7th, etc., harmonics are, respectively, (1.27/3)E, (1.27/5)E, (1.27/7)E, etc. The amplitude of the square pulse equivalent to the spectrum of Fig. 4b is 1.27E multiplied by $\pi/4$, or E.

When this square pulse is used to modulate the usual sinusoidal wave, the fundamental frequency of the modulated wave is superimposed on this plot at zero frequency. Sum and difference frequencies then appear on either side of the modulated frequency and a mirror image of Fig. 4b appears to the left of this chart with negative frequencies; that is, frequencies that are subtracted from the modulated frequency. This is in agreement with the superposition theorem [3]. Briefly, this theorem states that the spectrum of an amplitude-modulated wave (having any envelope) is identical with the spectrum of its own envelope, except that the amplitude-modulated wave is symmetrical about the carrier frequency and the modulation envelope is symmetrical about zero frequency.

Some authors prefer the method of presentation of Fig. 4c, which shows negative numbers--hence negative frequencies--to the left of zero on the abscissa. Because both plots furnish the same information, a choice may be made on the basis of individual preference.

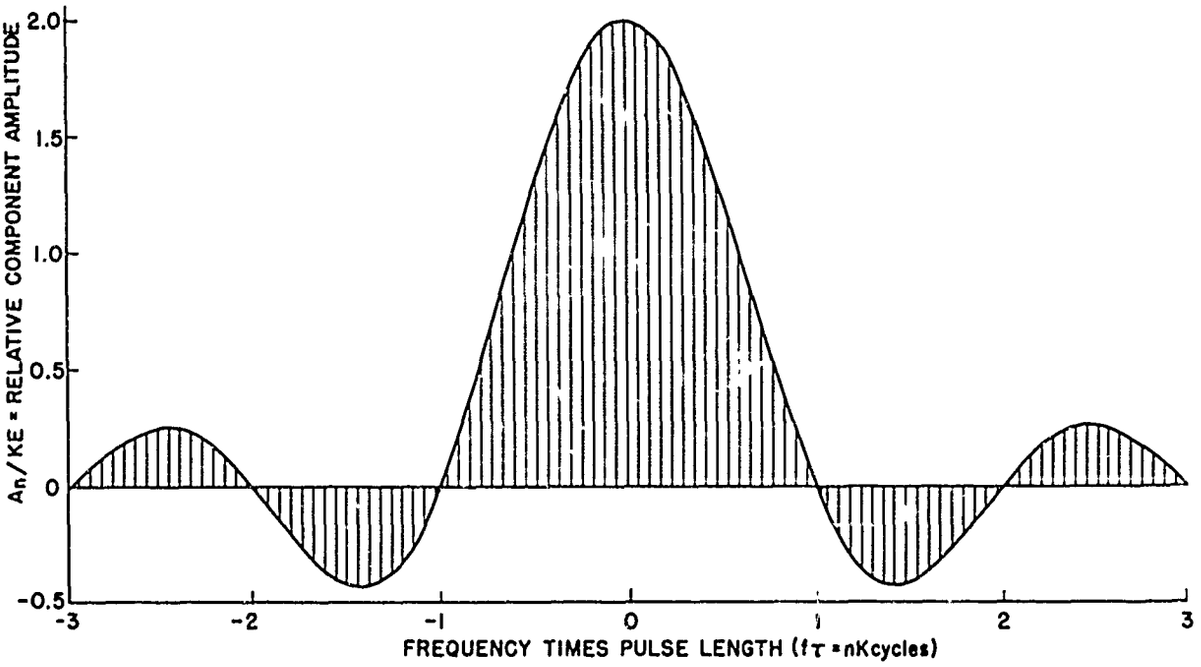

Fig. 4c. Normalized plot of the Fourier spectrum for square pulses, using the concept of negative frequencies. For pulses of Fig. 4a, the spacing of the vertical frequency lines represents 60 cps.

Spectral frequencies for the half-cosine and cosine-squared pulses are plotted in Figs. 5 and 6 for comparison with the square pulse spectrum of Fig. 4b. Attention is called to the decreasing importance of the harmonics and the increasing bandwidth of the major lobe as the rise and decay times of the pulse lengthen.

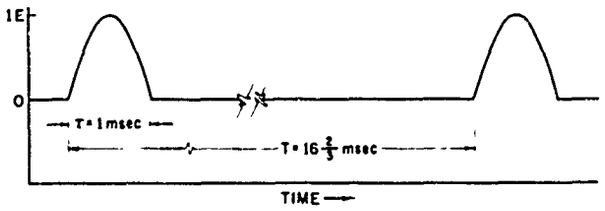

Fig. 5a. Half-cosine pulses at the repetition rate 60 pps.

The major lobe of the cosine-squared pulse of Fig. 6b is strikingly similar to the probability curve, $\exp(-x^2)$. A composite plot of the three spectra is presented in Fig. 7 using the concept of negative frequencies.

For easier mathematical manipulation, some authors, for example, Cherry [3], prefer to describe a pulse as composed of both positive and negative frequencies. In elementary a-c theory, sinusoidal quantities are sometimes depicted as the projection of a rotating vector onto some fixed axis. This projection varies sinusoidally with time, so that the rotating vector may be regarded as the generator of a sine wave.

The vector is imagined as lying in the plane of a coil rotating in a uniform magnetic field, so that the projection of the vector gives at every instant the amplitude of the emf induced in the coil.

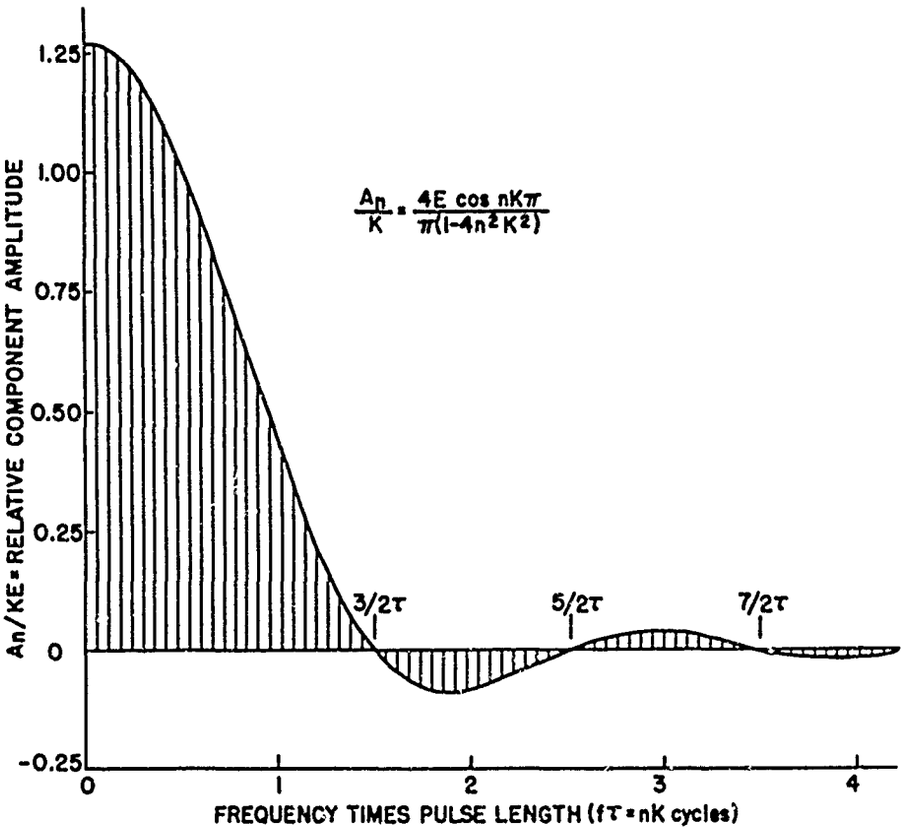

Fig. 5b. Normalized plot of the Fourier spectrum for half-cosine pulses. For pulses of Fig. 5a, the spacing of the vertical frequency lines represents 60 cps.

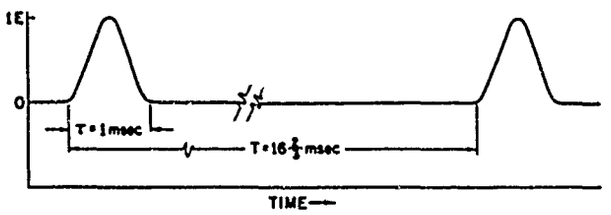

Fig. 6a. Cosine-squared pulses at the repetition rate 60 pps.

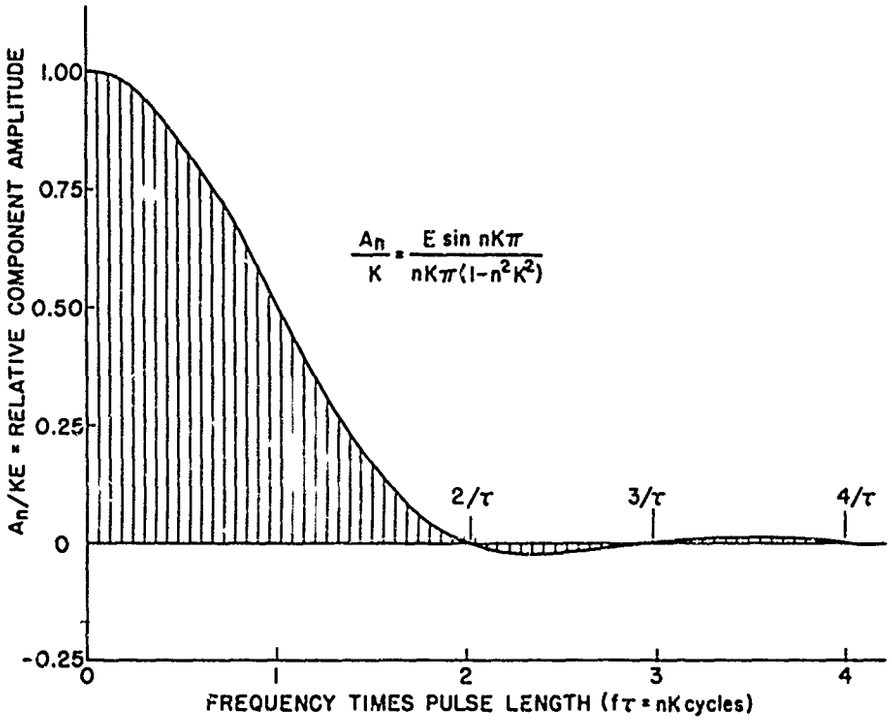

Fig. 6b. Normalized plot of the Fourier spectrum for cosine-squared pulses. For pulses of Fig. 6a, the spacing of the vertical frequency lines represents 60 cps.

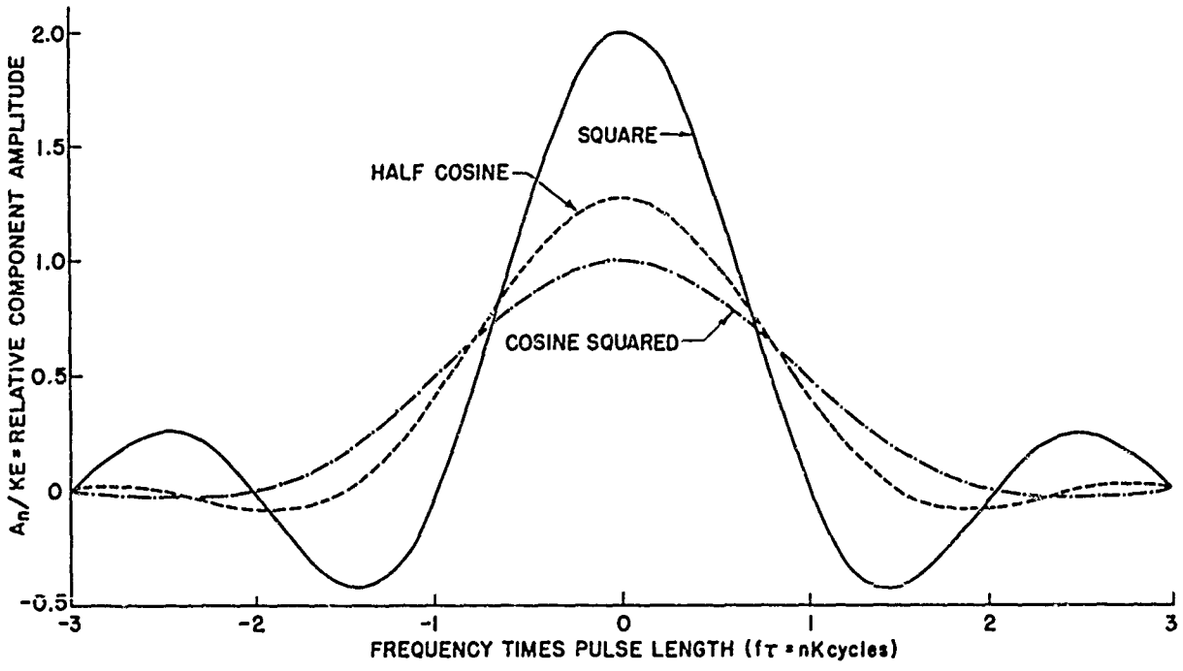

Fig. 7. Fourier spectra of square, half-cosine, and cosine-squared pulses.

Another and more logical way of depicting a-c vectors is to use a conjugate pair of vectors, each of which is half the length of the single vector, to maintain the proper amplitude. These half-length vectors are assumed to rotate in opposite directions at the angular speed ω, and the sum of their projections on the real axis varies sinusoidally, but the sum of the projections on the imaginary axis is always zero. Because these vectors rotate in opposite directions, their angular speeds must be $\pm\omega$, and this condition gives rise to the idea of "negative" frequency. The use of such negative values of frequency in calculations is quite legitimate and gives practical results, just as does the use of j or imaginary numbers in impedance analysis.

TREATMENT OF DATA

A communications channel must satisfy two essential conditions to make the waveforms of the input and output signals identical (apart from probable difference of level): The channel must be linear, and it must be completely nonselective with regard to frequency. When a given waveform is analyzed into a spectrum of sinusoidal terms, that particular spectrum (of amplitude and phase-angle components) is unique for that waveform. Hence, if the amplitudes or phases of these components are disturbed by selective circuits, the waveform of the output signal will be modified.

Sullivan [4] states: "The response of a network to a transient may be determined from a knowledge of the complete steady-state characteristics, if the amplitude and phase shift distortion of every (Fourier) sinusoidal component in the applied transient, imposed by the network's characteristics, be taken into account."

The calculation of transient response requires three discrete processes: (1) analysis of the applied transient into its Fourier spectrum; (2) modification of this spectrum according to the characteristics of the network; and (3) summation of all the component sinusoidal waves in this modified spectrum. Analysis of the transient has already been covered in some detail. The modifying process is dealt with in a later section. In this report, where a rectangular pulse modulates a sinusoidal wave, the phase shift distortion of every (Fourier) spectral component is neglected because measurements to determine this phase shift become exceedingly involved, and the computations become complicated and tedious. Also, the phase shift in the experiments was probably minimized by the narrow frequency range covered and could be neglected with an acceptable error. Only the amplitude distortion of the sinusoidal sideband components is considered. The calculations and experimental data are in reasonably good agreement, so this method of treatment seems justified. The amplitude of the center of the modified (and probably distorted) square pulse is obtained by arithmetic addition of the in-phase components above the abscissa and subtraction of the out-of-phase ones below. The sum approaches theoretical amplitude only when an infinite number of points is considered.

ESSENTIAL BANDWIDTH

The partial spectrum of a rectangular pulse modulating the carrier frequency 2.4 kc is shown in Fig. 8. The inclusion of much higher pulse harmonics than the fifth shown in the drawing would be necessary to approximate the true square wave in Fig. 3a. The absolute amplitudes of the spectral frequencies at 60-cps intervals are represented by the heights of the vertical lines, which were computed by multiplying the relative amplitudes by only $\frac{1}{2}K$ to compensate for the negative or lower sideband frequencies that are present below the carrier frequency. The circles of Fig. 8 represent the amplitudes of these frequencies as measured by a narrow-band harmonic wave analyzer. The values for frequencies below 540 cps defied accurate measurement, but most other values are in excellent agreement with theory.

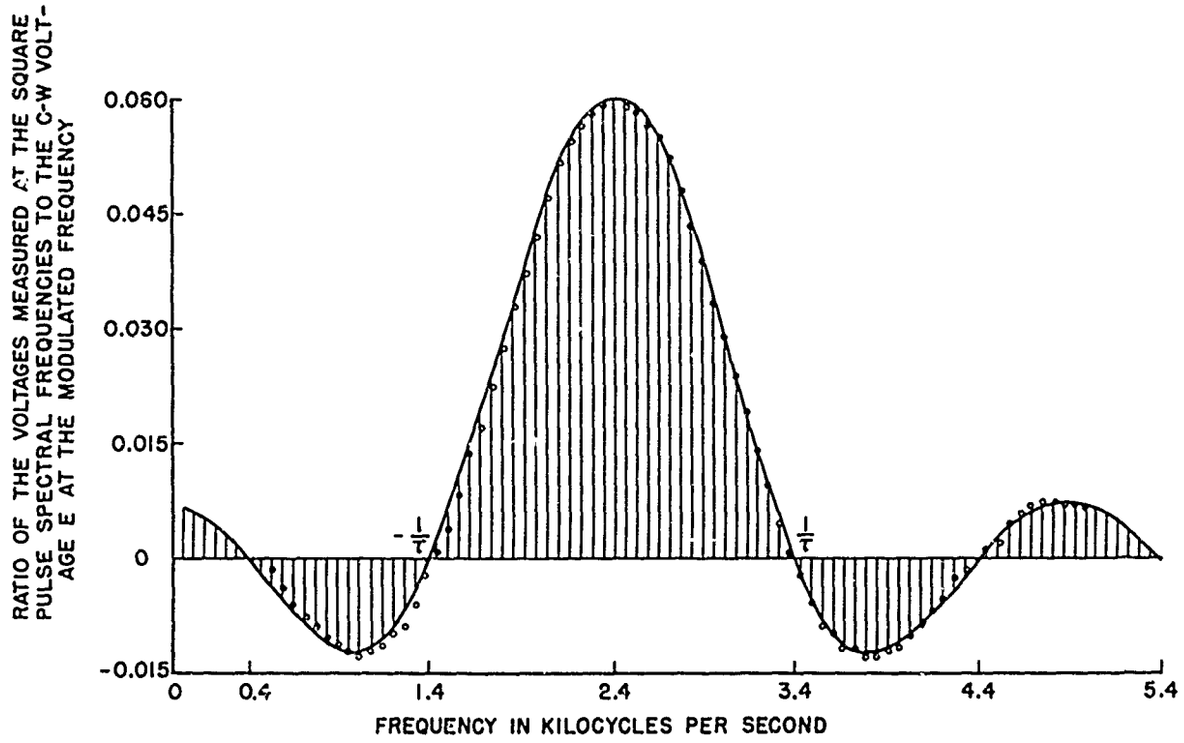

Fig. 8. Theoretical Fourier spectrum of a rectangular pulse modulating the frequency 2.4 kc, compared with experimental results.

The Appendix to reference [5] contains the statement: "A bandwidth equal to the reciprocal of the pulse length will produce some pulse distortion, although the energy in the pulse will be essentially the same as for a broad band system. Twice this bandwidth is sometimes called the essential bandwidth for pulse transmission." This is shown in Fig. 8 as the frequency band of 2 kc between $-1/\tau$ and $+1/\tau$ which includes only the primary frequency of the square pulse.

This definition of essential bandwidth probably originated in radar theory for search-type systems [6] and was transferred verbatim to acoustical calibration procedure. The design of radar systems had two requirements: (1) maximum signal-to-noise ratio, which occurs at a bandwidth only slightly less than $2/\tau$; and (2) highest peak signal voltage. The peak

amplitude of the modulating envelope is developed by eliminating all frequencies below $-1/\tau$ and above $+1/\tau$. There remains then only the primary sine wave shown in Fig. 3a, which apparently increases the amplitude of the envelope by 2 dB when compared with the square wave. When, however, a square pulse is used for modulation, a bandpass of $2/\tau$ increases the envelope only 1 dB. This amplitude is obtained by adding the spectral frequencies shown in Fig. 4b. For narrower or wider bandwidths, the expected amplitude changes depend on the positive or negative phases of the added bands of harmonic frequencies. For example, a bandwidth $1/\tau$ decreases the amplitude by 1.0 dB; a bandwidth $4/\tau$ decreases it by 0.9 dB; a bandwidth $6/\tau$ increases it by 0.5 dB. These are the levels only at the midpoint of the pulse, and are not necessarily the levels indicated by a peak-reading meter or recorder.

This possible increase in envelope amplitude is readily demonstrated by varying high-pass and low-pass filter cutoff values toward the modulated frequency. Peak amplitudes occur with the elimination of frequency bands outside $\pm 1/\tau$. A further narrowing of the bandpass to the band of frequencies $1/\tau$ causes the amplitude of the modulating envelope to decrease approximately 1 dB below the level of the square wave pulse. A decrease of like magnitude occurs for a resonant transducer driven with a pulse length of $(0.7Q + 1)$ cycles [7].

The bandwidth essential for retention of the original square pulse shape is infinite but, in most cases, a bandwidth ten times the so-called "essential bandwidth" is sufficient. That is, the bandwidth for negligible distortion of pulse shape should be twenty times the reciprocal of the pulse length [8].

When the signal frequency is modulated with the half-cosine pulse shape of Fig. 5, a bandwidth of only $3/\tau$ causes a positive 3% error in voltage measurements. When the bandwidth is decreased to $2/\tau$, the summation of the spectral frequencies of Fig. 5b shows the pulse amplitude to be decreased by 1 dB.

A similar analysis of the cosine-squared pulse shows that the bandwidth $4/\tau$ causes a positive error in pulse amplitude of only 1%, but that decreasing the bandwidth to $2/\tau$ decreases the pulse amplitude sufficiently to cause an error in measurement of 2 dB.

TECHNIQUE FOR MEASUREMENT OF SPECTRUM

All measurements of the spectral frequency amplitudes were made by the repeated pulse excitation of narrow-band filters at the repetition rate 60 pps. Two harmonic wave analyzers were used interchangeably, one manufactured by Hewlett-Packard Company and the other by General Radio Company. Some data were taken using the filter in an automatic transmission measuring system. The passbands ranged from 7 to 15 cps, which allowed complete separation and measurement of individual sideband frequencies. All measurements were relative, with surprisingly high accuracy over a 34-dB range as shown in Fig. 8, where the measured and calculated levels are compared.

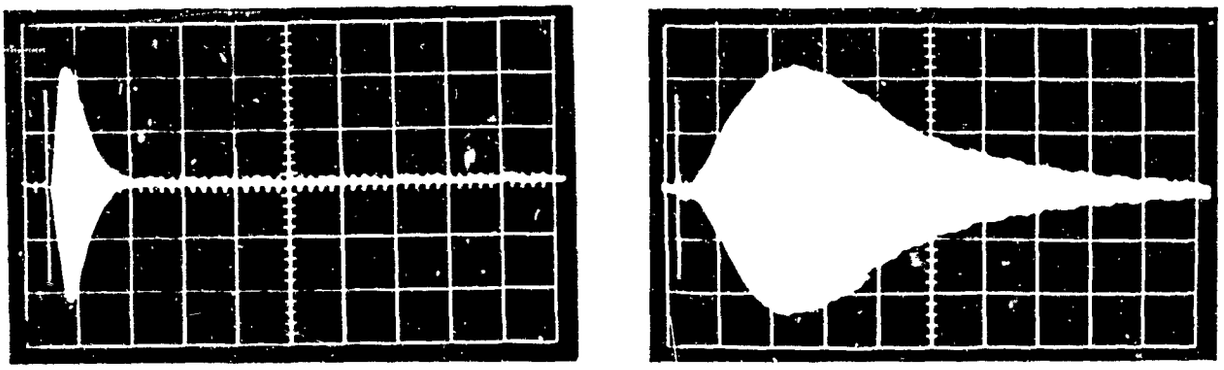

a. Wide passband setting. b. Narrow passband (Q = 343).

Fig. 9. Response of harmonic wave analyzer to a 1-msec pulse.

The buildup and decay of a single pulse examined at the output of a heterodyned multistage spectrum analyzer is of interest, if only academically. Figure 9 illustrates the variation in output signal with the maximum and minimum settings of the continuously variable passband in the Hewlett-Packard harmonic wave analyzer. Figure 9a shows the rise-decay envelope initiated by the 1-msec pulse that appears as a very narrow line located approximately two small divisions to the right of the first vertical line. Figure 9b shows identical conditions except for a narrowing of the frequency passband and a slight displacement of the pulse to the left. The oscilloscope sweep time for the pictures was 0.25 second, making the time between vertical marker lines 25 msec. The discussion that follows applies to both figures, but only Fig. 9b will be used as an example of phase delay, because of the larger time lapse between the input pulse and the maximal amplitude of the output of the analyzer.

The picture shows that the analyzer output is virtually zero for 5 msec after the pulse has been applied to the input. It also shows that the maximal output does not occur until 50 msec later. This retardation is similar to that occurring in multistage amplifiers where the output response signal remains substantially zero for a very long time and then starts to build up as though the wavefront has a definite (virtual) speed through the amplifiers. The maximal output is the buildup of the modulated fundamental frequency and shows the greatest delay. The 45 milliseconds prior to this maximum contain the sideband frequencies above and below the center frequency, consequently show less retardation and more attenuation. The calculated Q of the wave analyzer was 343. This figure is the quotient of the operating frequency, 2400 cps, divided by the bandpass, 7 cps. This computation follows from one definition [5] that states: "Q is the ratio of the system's resonant frequency to the frequency interval between its quadrantal or half-power frequencies..." Further, "...Q is a measure of the duration of the transient and is used in specifying the build-up or decay time of the resonant system under pulsed excitation conditions."

The voltage or current decay in a resonant electrical circuit usually is expressed as [9]:

$$A_t = A_i \exp(-Rt/2L),$$

where A_t = amplitude at time t, A_i = initial amplitude, R = circuit resistance, and L = circuit inductance. Without revision, the negative exponent in this expression does not lend itself well to acoustical computations. If both numerator and denominator of the exponent are multiplied by πf, the result is

$$\pi fRt/(2\pi fL) = (R/X)\pi ft,$$

where $R/X = 1/Q$, and ft = number (n) of cycles.

The formula for the transient decay then becomes

$$A_t = A_i \exp(-\pi n/Q),$$

and the transient buildup is obtained by subtracting A_t from one. As an example: when $n = Q$, $\exp(-\pi) = 0.04$, and the pulse amplitude during this period either has decayed to 4% or has built up to 96% of its steady-state level.

When $n = 1$, the exponent π/Q is called the logarithmic decrement (log. dec.) of the circuit and is designated by the symbol δ. It represents the ratio of successive maxima of the current in an oscillatory discharge.

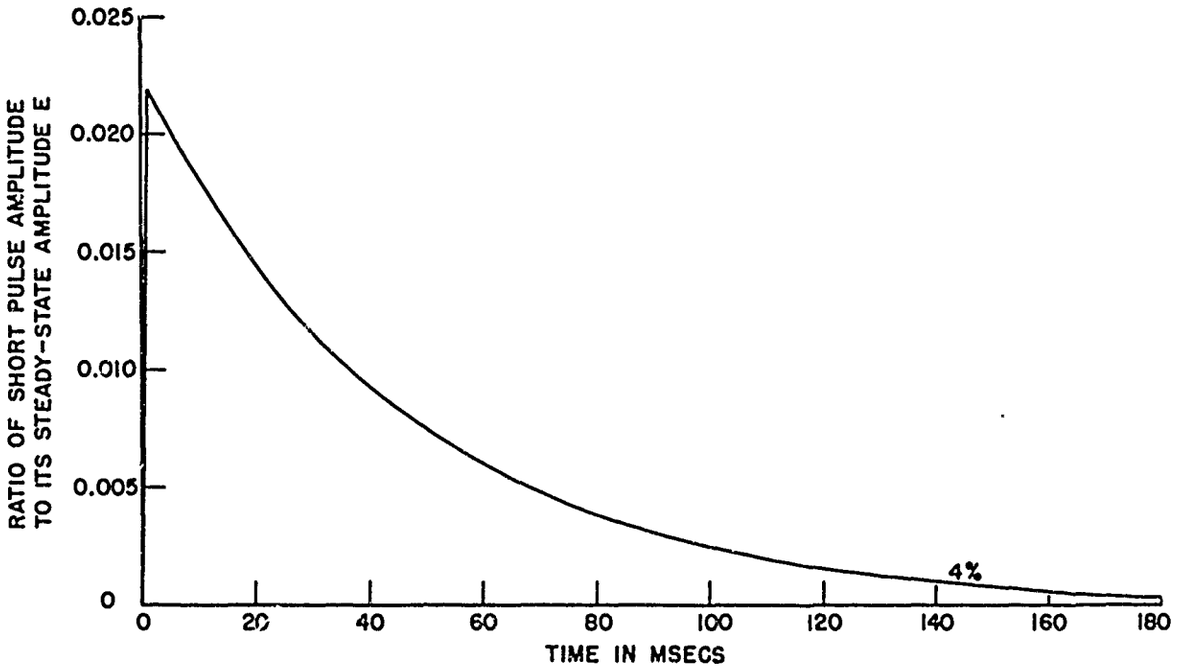

Fig. 10a. Comparison of rise and decay times in a high-Q circuit.

A theoretical curve comparing the rise time with the decay time of a 1-msec pulse at the frequency 2400 cps, with a circuit Q = 343, is shown in Fig. 10a. The pulse has decayed to 4% of its peak (not steady-state) amplitude in 143 msec (Q/f seconds), although the buildup time was only 1 msec. The buildup time exactly equals the decay time only after the pulse has attained steady state, which theoretically is never reached, but is only approached asymtotically. In general practice, the steady-state condition is assumed to exist after a period equal to Q cycles.

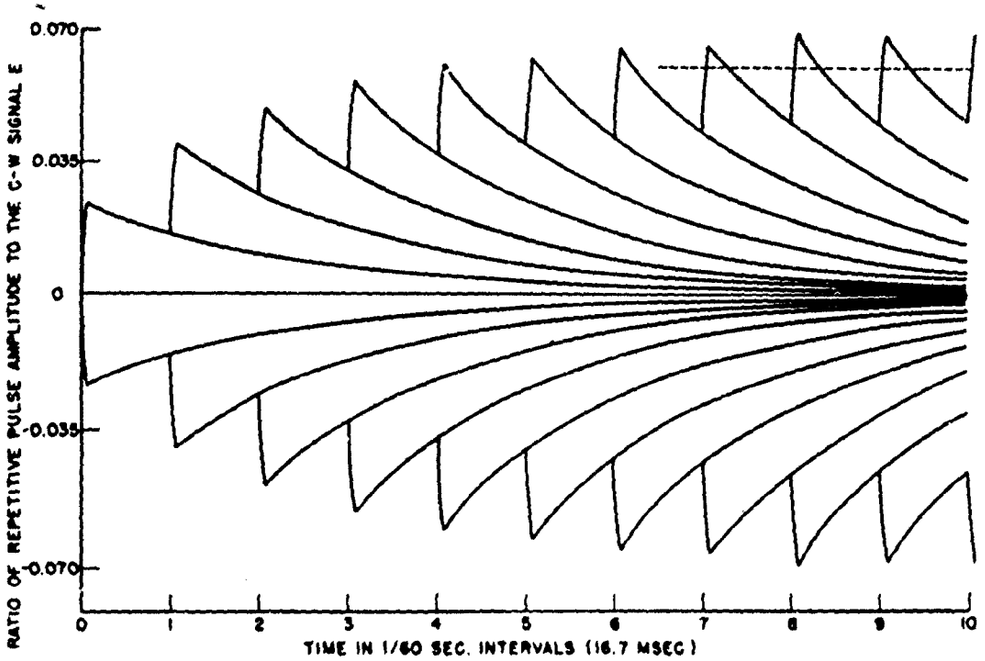

Fig. 10b. Buildup of repetitive 1-msec pulses to steady state in a circuit of Q = 343.

The large time constant or long signal-storage time of a high-Q circuit permits the summation of repetitive short pulses when the output of an oscillator is gated to maintain a constant cyclic phase relationship. A graphical representation of the buildup to steady state of repetitive 1-msec pulses at the rate 60 pps in a circuit of Q = 343 is shown in Fig. 10b. The ordinate is labeled so that the average pulse amplitude can be compared directly with a c-w signal when measured by the same wave analyzer. The average pulse amplitude represented by the horizontal dashed line in the upper right-hand corner of the chart shows the condition where the buildup of an individual pulse in 1 msec exactly equals the decay of the preceding pulse in 1/60 second.

The average of the peaks and valleys of this sawtooth wave shows this quasi-stable state to be approximately 24.3 dB below the c-w signal level, whereas actual measurements showed it to be 25.5 dB lower. The prediction from the theory is that the difference should be 24.5 dB (≈ 20 log K), which makes this graphical representation appear reasonable. The inertia of a meter movement or a recorder pen was sufficient to produce a steady reading between the bottom and the peak of the sawtooth wave.

This same method of spectrum amplitude measurement was described in [10] for the harmonic analysis of repetitive transients with graphical input data.

The peak voltage at the 9th pulse may be computed from the expression:

$$E_9 = (1 - e^{-2.4\delta})[1 + e^{-4\delta} + e^{-2(4\delta)} + e^{-3(4\delta)} + \ldots + e^{-8(4\delta)}]$$

The first expression in parentheses is the amplitude level of the 1-msec pulse at the frequency 2400 cps. The second expression is the sum of the pulses after they have decayed for subsequent periods of time.

The abscissa in Fig. 10b is divided into time intervals equal to the reciprocal of the repetition rate and designated as T earlier in this report. Between the 8th and 9th intervals, a quasi-steady state condition is approached. Particular attention is called to this occurrence because the buildup has been attained with far fewer than the Q cycles that theory predicted were necessary; in fact, with n = KQ cycles. If ft (frequency times time) is substituted for n cycles, the formula again becomes applicable, because 2400 x 9/60 is approximately equal to the circuit Q. The foregoing warns that a high-Q circuit approaches a quasi-steady state in a time interval that would contain Q number of cycles with c-w although the actual number of cycles present may be far less than Q, because the signal during the buildup time is a series of short pulses.

FREQUENCY SHIFT OF SPECTRUM, CALCULATED

When the pulse whose spectrum is shown in Fig. 4b is centered on a rising response curve (response level increasing with frequency, as when measuring below the resonant frequency of a transducer), the upper sideband frequencies are amplified more than the fundamental and become predominant for an ungated peak-reading detector. ("Ungated" measurement is defined as the measurement of a pulse in its entirety; it is not sampled by a receiving gate of shorter length than the pulse.)

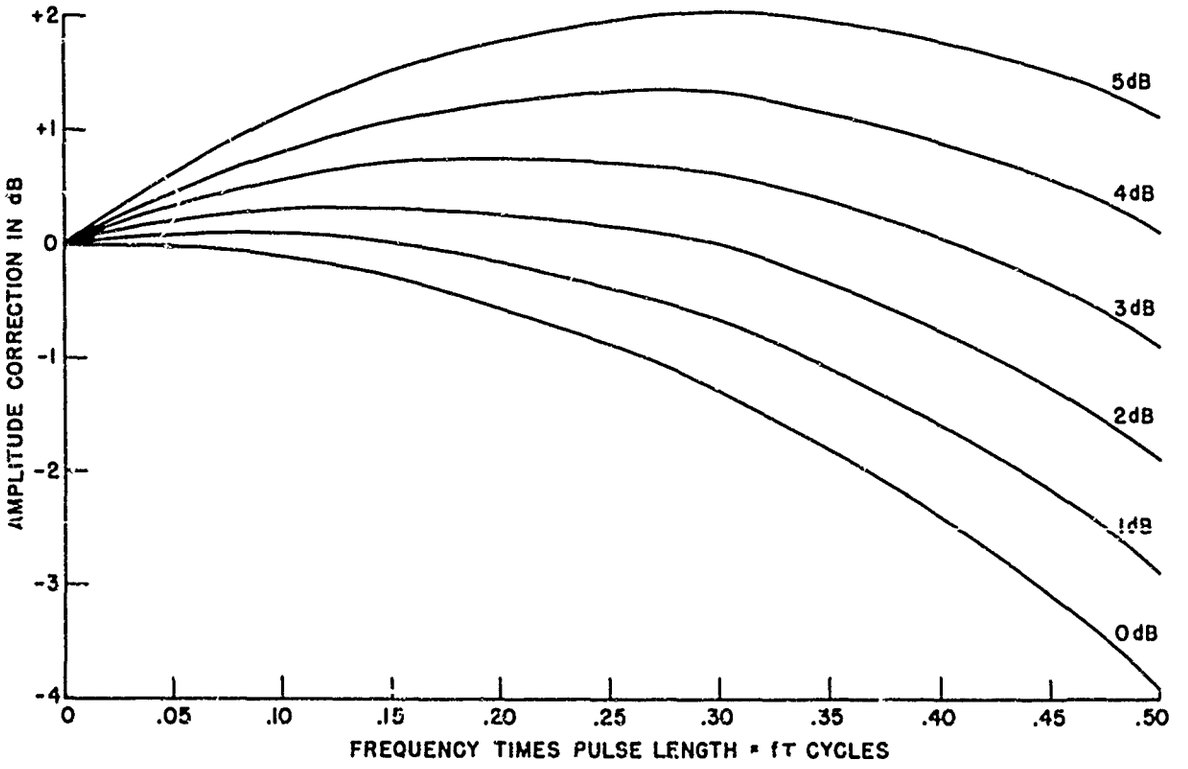

Fig. 11. Normalized curves for changes in amplitude and displacement of spectral frequencies for a square pulse with asymmetrical sideband amplification. Curves are for response increases of 0 to 5 dB.

Figure 11 shows normalized curves for both the spectral frequency displacement and the spectral amplitude when the rectangular pulse wave is subjected to varying degrees of asymmetrical sideband amplification. The lowest curve is the upper portion of the main lobe of Fig. 4b, extending from the amplitude 2E at zero frequency to approximately 64% of 2E at $f\tau = 0.5$. The curve is expanded in length for increased legibility, and the ordinate is plotted in decibels to simplify its use. For the bottom curve, the network's characteristics are flat; the slope is 0 dB. On a falling response curve (response level decreasing with frequency, as when operating above the resonance of a transducer) a mirror image of these curves would appear to the left of zero.

The abscissa is the product of frequency and pulse length. This method of presentation normalizes the curve for any length of pulse. The frequency band is obtained by dividing the length of the abscissa as labeled by the length of the pulse in seconds; frequency = $0.5/\tau$. The curves labeled from 0 to 5 dB give the increases in spectral amplitude over the frequency band shown.

For a 1-msec pulse the entire abscissa length of Fig. 11 becomes $0.5/0.001 = 500$ cps. When this pulse exists on a slope that rises 2.5 dB in 500 cps, imagine a curve midway between the curves for 2 dB and 3 dB. The maximum on this interpolated curve lies at the point (150 cps, 0.5 dB), and indicates that the pulsed fundamental frequency has been shifted to the adjacent spectral frequency of greatest amplitude and higher than the fundamental by 150 cps, and that some spectral lines have been increased in level by 0.5 dB. A transmitted rectangular pulse wave modulating the frequency 2400 cps, whose partial spectrum was shown in Fig. 8, would be received at the frequency 2550 cps. The increase in amplitude level of the ungated pulse would probably exceed 0.8 dB. This value would be computed by the addition of all the spectral frequencies shown in Fig. 12, which represents the distorted spectrum.

The foregoing method applies equally well to a slope of opposite sign, where the response level decreases with frequency. Then, however, curves may be visualized as shifting the maximal spectral amplitude of Fig. 8 to a lower frequency. The amplitude of the spectral frequencies would still be increased by 0.5 dB, but the pulse would be received at the lower frequency 2250 cps.

The frequency is increased on a positive slope and decreased on a negative slope. At the peak of the curve (point of inflection) the circuit or transducer has the characteristics of a band-pass filter.

FREQUENCY SHIFT OF SPECTRUM, EXPERIMENTAL

Two available transducers (types J9 and XQB) having a combined positive response slope with increasing frequency were rigged 2 meters apart at 3 meters depth in open water. The type J9 was driven with sixty 1-msec pulses per second at the frequency 2.4 kc.

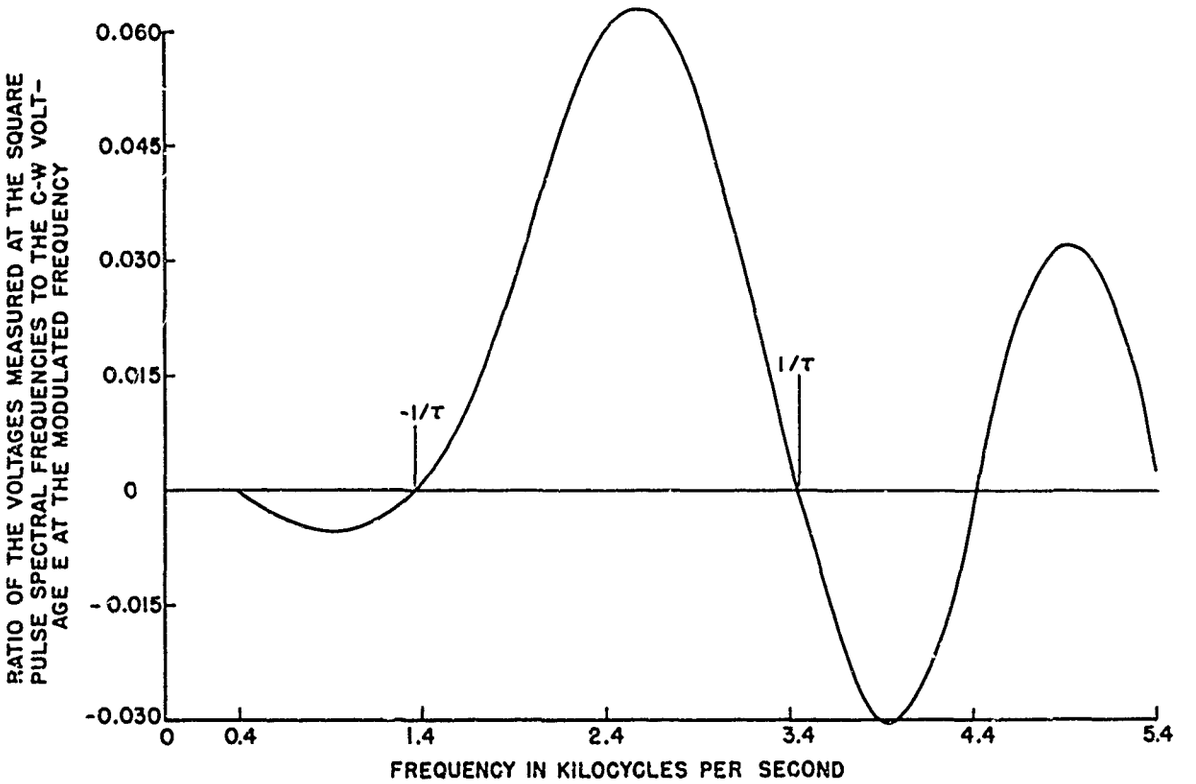

Fig. 12. Fourier spectrum of Fig. 8 modified by response slope 2.5 dB per 500 cps.

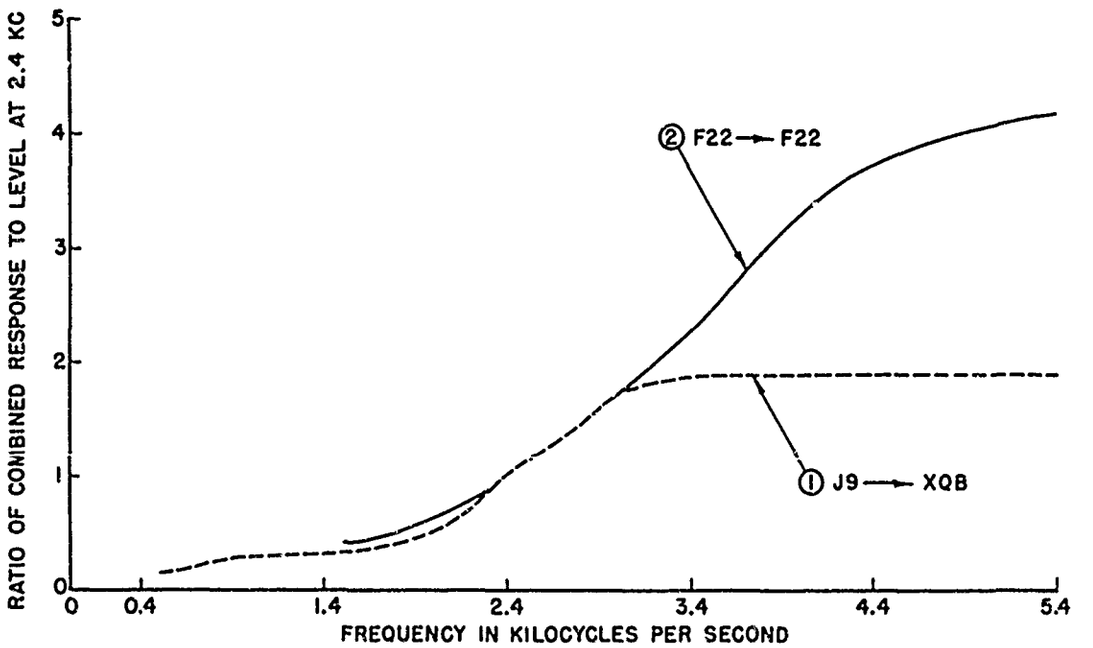

Fig. 13. Combined transmitting-receiving responses of two pairs of transducers used experimentally.

The combined response of the two transducers is shown by curve (1) in Fig. 13, with the voltage amplitudes plotted relative to the response measurement obtained at 2.4 kc. The curve shows a positive slope of 1.55 from the reference frequency to the frequency 500 cps higher. That is, the combined response is 3.8 dB higher at 2.9 kc than at 2.4 kc.

The received spectral frequency output from the measuring hydrophone was recorded at 60-cps intervals with a narrow-band filter over a range sufficient to show the frequency displacement of the pulse spectrum and the increased amplitude of the harmonic frequency bands. From the curve of Fig. 11, a spectral frequency shift of 250 cps is to be expected for a 1-msec pulse. This theoretically predicted shift is in agreement with the 240 cps shown by curve (1) of Fig. 14. Summation of all the spectral frequencies enclosed by the curve yields an increase of 1 dB in the amplitude of the pulse, whereas the normalized chart predicts 1.2 dB. This discrepancy probably is caused by the flattening of the combined response curve above 3 kc. This flattening permits the upper harmonic bands to be far less distorted than if the curve had continued its steep upward slope.

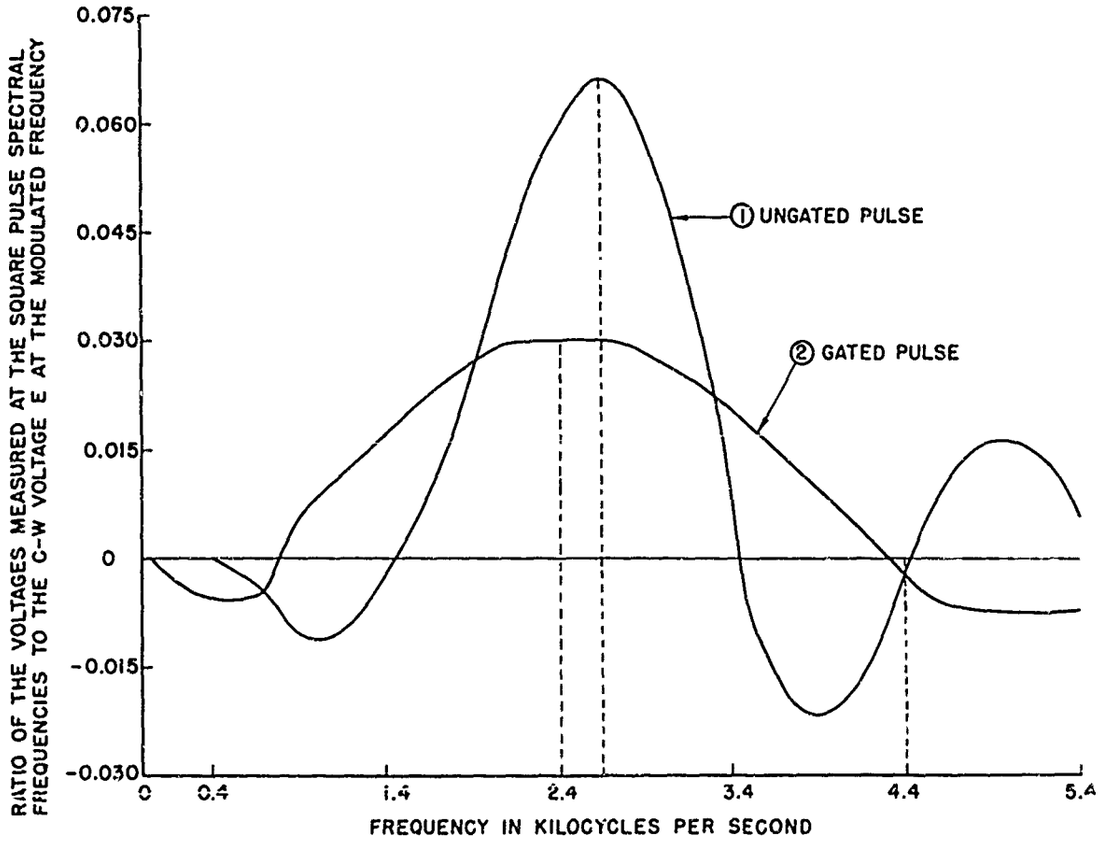

Fig. 14. Spectra of ungated and gated pulses with asymmetrical sideband amplification.

Curve 2 of Fig. 14 shows the result of gating the 1-msec transmitted pulse by a 0.5-msec received pulse so that only the central portion of the transmitted pulse is used in the measurement. Thus, the distortion terms appearing at the leading and trailing portions of the pulse were eliminated. The frequency displacement is then barely discernible, and the summation of all the spectral frequencies indicates zero error in amplitude at the pulse center.

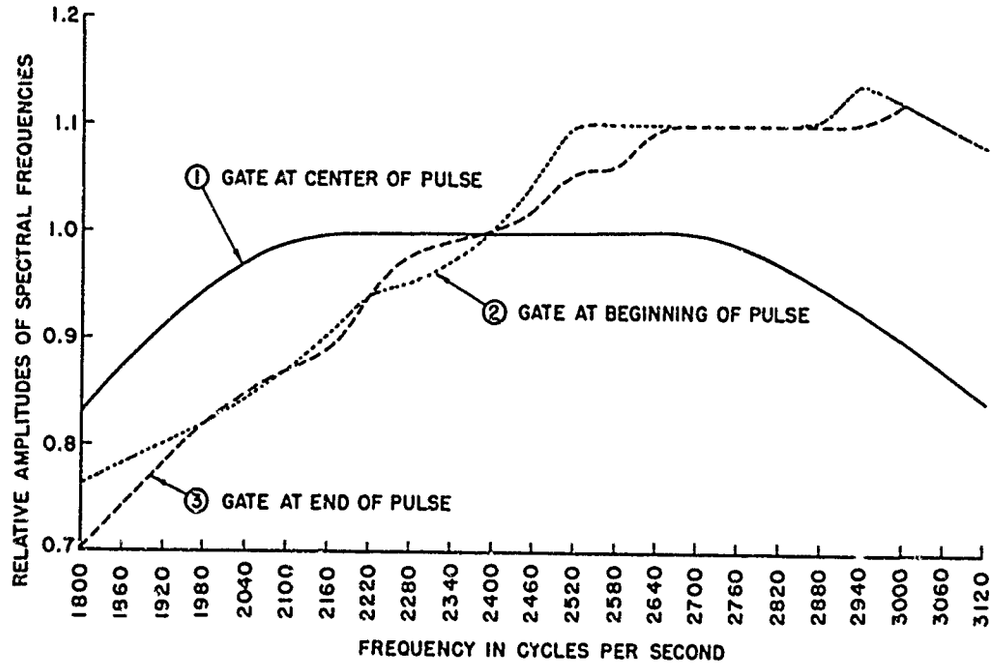

Fig. 15. Spectral frequency content of various portions of a pulse with asymmetrical sideband amplification.

The frequency and amplitude scales of Fig. 14 are expanded in Fig. 15 to show the location of the spectral frequencies in the pulse that cause the frequency displacement. Curve (1) is the peak of the 0.5-msec received pulse shown as curve (2) of Fig. 14; it demonstrates the nearly perfect symmetry obtained above and below the center frequency 2.4 kc. Curves (2) and (3) of Fig. 15 result when the gate is moved so as to sample the beginning and the end, respectively, of the pulse; they show the equality of the amplitude-distorted spectral frequencies.

The oscillograms in Fig. 16 show the distortion of the pulse and the location of the gate for the measurements of Fig. 15. The vertical graticule lines represent time intervals of approximately 0.167 msec. The presence of the high-frequency components is readily recognized by the short wavelengths at the beginning and end of the pulse as shown in the upper and lower traces.

This experiment was repeated with two type F22 transducers currently used in the anechoic tank for low-frequency reciprocity calibrations. Their combined response level plotted relative to their level at 2.4 kc is shown by curve (2) of Fig. 13. Measurements were made as previously described except that the pulse repetition rate was doubled, which spaced the spectral frequencies at 120-cps intervals and doubled the magnitude both of K and the absolute components. The resulting measurements of the entire pulse and of the gated pulse, plotted in Fig. 17, show striking similarity to those of Fig. 14. Greater care was exercised in this second experiment to obtain more nearly exact pulse lengths of 0.5 and 1 msec. This exactness is demonstrated in Fig. 17 by the crossover at 4.4 kc of the two curves at zero level. That is, the first zero crossing for the 0.5-msec pulse is at the same frequency as the second zero crossing for the 1-msec pulse.

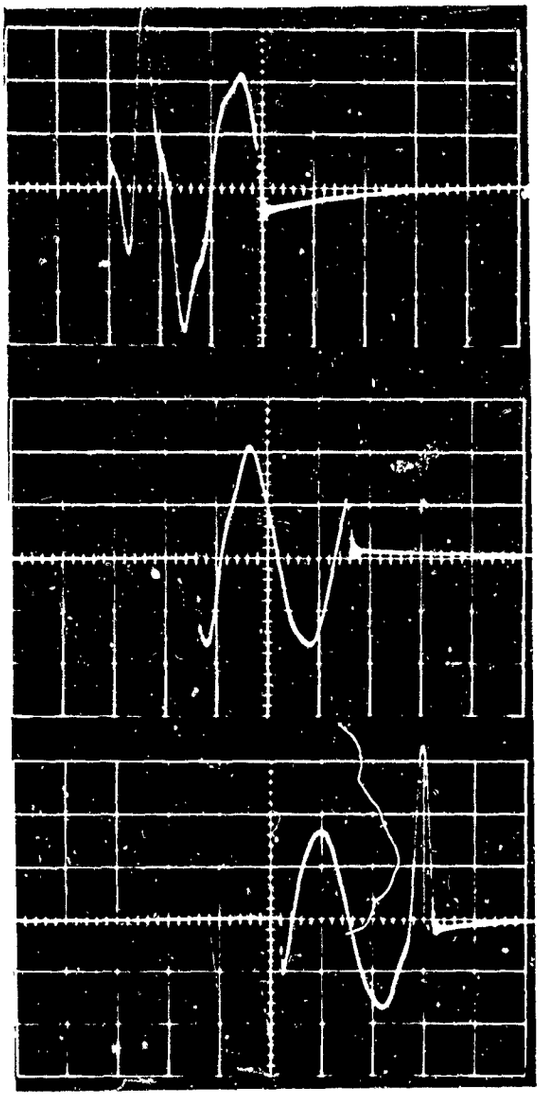

Fig. 16. Variation in 0.5-msec gating of a 1-msec pulse at 2.4 kc. Grid length = 1.67 msec.

Summation of the amplitudes of the spectral frequencies in the ungated 1-msec pulse again indicates an error of +1 dB in the amplitude of the square pulse. This error is eliminated in the lower of the two curves where the pulse was gated at its center. Once again it is demonstrated that properly gating the pulse eliminates the frequency displacement caused by the sloping response characteristic.

COMPARISON CALIBRATIONS USING SIDEBANDS

A study of Fig. 8 revealed the possibility of using a particular spectral frequency in a lower harmonic of a rectangular-wave modulated frequency for the sound source in the comparison calibration of a non-resonant hydrophone. This method would allow the use of short pulses at low frequencies, thus eliminating sidewall reflections that would occur with c-w transmission. These lower frequencies cannot ordinarily be pulsed, because each pulse may then contain only a fraction of a cycle. By lowering to 2.0 kc the modulated frequency 2.4 kc shown in Fig. 8, however, the higher-amplitude spectral frequencies in the first lower harmonic could be shifted downward to approximately 500 cps. It would

then appear feasible to use this lower frequency as the sound source. A fundamental or carrier frequency of 500 cps cannot be used with the pulse length 1 msec because the pulse would then include only half a cycle.

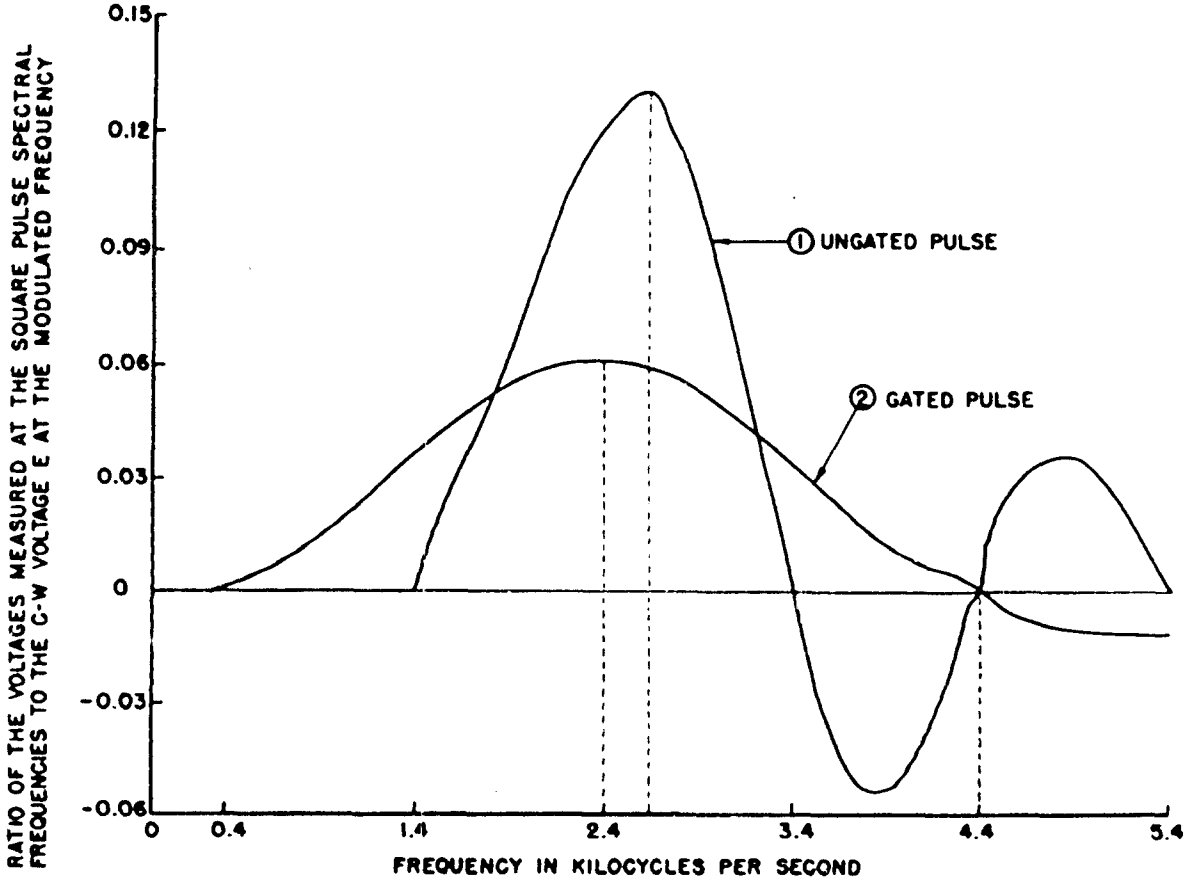

Fig. 17. Spectra of gated and ungated pulses with asymmetrical sideband amplification.

A 1-msec pulse at the frequency 2 kc, the repetition rate 60 pps, and the available power 50 watts was used to drive a type J9 projector. A standard and an unknown hydrophone were spaced one meter from the projector and their sensitivities were compared by measuring the amplitude of spectral frequencies in the lower square wave harmonics. The method of measurement was the same as described under "Technique for Measurement of Spectrum." The voltage sensitivities of the two hydrophones differed by as much as 30 dB. The received pulse was gated and its length made equal to that of the transmitted pulse. This left the location of the harmonic frequency maxima undisturbed, and eliminated reflections. The driving frequency was adjusted to obtain identical incremental changes of a particular spectral frequency, which always remained at a fixed frequency interval below the driving frequency.

At 450 cps, the sideband calibration was 1 dB lower than the c-w calibration made just prior. Between this frequency and 1000 cps, the two methods were in disagreement by no more than 0.6 dB. Frequencies below 450 cps consistently showed errors as large as 6 dB, thus setting 450 cps as the lower frequency limit for the sideband method for a 1-dB variation from c-w results. Equally good results were obtained by using a 0.5-millisecond pulse and a driving frequency near 3.5 kc. This method makes

feasible comparison calibrations of nonresonant transducers in the high-pressure tank down to the frequency 450 cps without sidewall reflections. During the measurements, some "jitter" of the meter needle of the harmonic wave analyzer was observed. This jitter was reduced considerably by doubling the pulse repetition rate to 120 pps.

TRANSDUCER Q_e AND Q_m DEFINED

The values of Q associated with an electroacoustic transducer are understood only vaguely by many persons engaged in underwater sound evaluations. This is not always the fault of the individual. A literature search shows that the culpability lies with authors whose definitions are inexplicit, confusing, partially true, or completely false. The following explanation is an attempt to give the reader a feeling for Q by explicit definitions of what it is, together with some excerpts from other authors to clarify what it is not. Probably exception can be taken to some statements that follow, but it is hoped that the exceptions will be rare.

The Q associated with an electroacoustic transducer is not a unique value; the transducer possesses both electrical (Q_e) and mechanical (Q_m) properties. These two Q's will be defined and discussed individually, although it should be borne in mind that their product is used as a parameter in the design of transducers.

According to [5], the electrical Q (Q_e) of a transducer specifies the magnitude of the ratio of the electrical reactance to the electrical resistance (series circuit), or the magnitude of the ratio of the electrical susceptance to the electrical conductance (parallel circuit) at the frequency of mechanical resonance. And, [11] Q_e is a parameter of the circuit defined as the quotient of the shunt resistance divided by the shunt reactance (parallel circuit) at the resonant frequency only. It is a crystal constant whose value depends on:

(1) Crystal material
    (a) sound velocity in
    (b) piezoelectric constant of
    (c) dielectric constant of

(2) Type of drive
    (a) clamped
    (b) symmetric
    (c) inertia

(3) Load medium
    (a) water
    (b) air
    (c) other

A popular misconception is that the value of Q_e can be determined readily at any particular frequency of interest by measuring the complex impedance at that frequency. It is, of course, possible to measure the ratio of reactance to resistance at any frequency and this ratio may be useful for some purposes, but it is not the Q_e of the transducer except at mechanical resonance.

According to both Hunt [12] and Vigoureux [13], the mechanical Q (Q_m) of a transducer "is most fundamentally significant as an expression of the ratio of the peak value of the mechanical energy stored during a cycle to the total energy dissipated in a radian period, that is, in a time interval $1/\omega$." Q_m specifies the sharpness of mechanical resonance and is a measure of the transient duration in either the buildup or decay time under pulsed excitation with a specific electrical termination and acoustic load.

As with Q_e, the Q_m of a piezoelectric transducer may be computed from the material on page 106 of reference [8] or page 176 of reference [11], where it is tacitly assumed that the proper driving impedance is used. Reference [8] mentions the unreliability of computed values, where the error may approach the factor 2. The original article quoted by this reference gave the theoretical value $Q_m = 16$ and the corresponding experimental value $Q_m = 9$. The difference was attributed to losses in the mounting. Re-examination of the data in [14] showed a theoretical $Q_m = 15$ and a measured $Q_m = 10$ obtained with an unmounted barium titanate transducer. This result switched the hypothesis from "mounting losses" to the "numerous approximations in the formula." These discrepancies do not justify recommending that the value of Q_m be theoretically calculated rather than measured.

The number of suggested methods for obtaining the value of Q_m from measurements is myriad. Apparently, the same confusion exists about determing Q_m as was found in defining Q_e. Some writers hold that, inasmuch as there are a number of frequency responses (voltage receiving, current receiving, transmitting current, transmitting voltage, etc.) associated with a particular transducer, there is a measurable value of Q_m corresponding to each frequency response curve. This statement is again in disagreement with the definition in [5], "The appropriate response-frequency curve for the selection of the resonant frequency is that one in which the excitation, electrical or acoustical, varies with frequency in such a way that the driving force exerted on the mechanical system is constant and the observed quantity is one which is proportional to the velocity in the mechanical system." This states without qualification that the Q_m of a particular class of transducer may be obtained only from specific curves or observations applicable to that type of transducer. It is admitted that a number to represent Q can be obtained from almost any available plot, but it is not the mechanical Q (Q_m).

It is recommended that the final sentence in section 4.6 of [5] read: "In specifying a mechanical Q, the nature of the electrical termination must be stated, i.e., the termination must be an open circuit or a short circuit, depending upon the nature of the electromechanical coupling." The definition states that Q_m can be determined only when the transducer is electrically driven with constant voltage or current, or mechanically driven with zero or infinite terminating load impedance for that particular class of transducer. The specification of "short circuit" or "open circuit" for the electrical termination appeared in the final corrected draft of the American Standard, but was inexplicably deleted only a few months prior to printing.

The equations defining Q_e and Q_m show that the electrical Q increases with increased loading (ρc), and the mechanical Q decreases with increased loading. For example, the Q_m of a quartz transducer is 50,000 when the load is air (ρc = 42 g/cm^2 sec) and only 15 when the load is water (ρc = 150,000 g/cm^2 sec). This inverse direction of change of electrical Q with loading leads to the conclusion that the buildup time of the pulse is unaffected by Q_e except for an exponentially decaying d-c component that is added to the exponentially increasing sinusoidal current or voltage wave. This d-c component displaces the first few cycles of the pulse above or below the zero-reference line and its magnitude depends upon both Q_e and the phase of the cycle at the time the pulse is started. An oscillographic observation of repetitive pulses starting with the usual random phase may show that the first few cycles have a wagging motion. The d-c component is discussed by Kerchner and Corcoran [15].

When controllable, Q_e should be kept to a minimum to insure the least possible change in the relative amplitude and phase of the pulse throughout its frequency spectrum. That is, the driving amplifier should "see" a load having minimal asymmetry.

The experimental determination of Q_m for the electrostatic (piezoelectric) class of transducers requires test conditions (or data plots) different from those for the electromagnetic (electrodynamic or magnetostrictive) class. Because it is necessary to treat the classes individually, discussion and comments are limited; only the most frequently used methods are discussed, and mathematical proof that is available in texts is omitted.

The Q_m of a piezoelectric transducer is obtained from:

(1) Transmitting VOLTAGE response.
Comment--The resonance frequency is divided by the frequency band between the 3-dB-down points on the curve. The probable error is less than 20%.

(2) Free-field CURRENT sensitivity (short circuit).
Comment--Same as (1).

(3) Motional ADMITTANCE circle.
Comment--The frequency at the diametral intersection of the circle (resonant frequency) is divided by the difference in the quadrantal frequencies. The latter frequencies are determined at the points on the circle where it is intersected by a second diameter drawn perpendicular to the first one. The probable error is less than 20%.

(4) Motional ADMITTANCE circle.
Comment--$Q_m = \frac{1}{2} f_0 (d\theta/df)$; $f = f_0$, where f_0 is the resonant frequency and θ is the phase angle in radians. This relation is defined in [5] as "one-half the rate of change at resonance of the phase angle of the system's ADMITTANCE with incremental change in the ratio of the frequency to the resonance frequency."

Because the data are the same as in (3) above, the value of Q_m is virtually the same. This method is not recommended because it involves additional computations.

(5) Cyclic buildup or decay of acoustic pulse.
Comment--The driving amplifier must furnish CONSTANT VOLTAGE. Hydrophone should be of nonresonant type. Q_m equals the number of cycles shown on the oscilloscope between the initiation of the pulse and the point where the amplitude attains 96% of its steady-state value, or decays from steady state to 4% of that value. The error is less than 5%.

The Q_m of the electrodynamic or magnetostrictive transducer is obtained from:

(1) Transmitting CURRENT response.
Comment--Same as (1) for piezoelectric type.

(2) Free-field VOLTAGE sensitivity (open circuit).
Comment--Same as (2) for piezoelectric type.

(3) Motional IMPEDANCE circle.
Comment--Same as (3) for piezoelectric type.

(4) Motional IMPEDANCE circle.
Comment--Same as (4) for piezoelectric type, except change the word ADMITTANCE to IMPEDANCE in the definition.

(5) Cyclic buildup or decay of acoustic pulse.
Comment--Same as (5) for piezoelectric type, except the driving amplifier must furnish CONSTANT CURRENT.

SONAR TRANSDUCER Q, EXPERIMENTAL

Elementary resonant circuit theory, which teaches that pulse buildup and decay times are functions of the Q of the entire circuit and are not uniquely dependent on the Q of the load, is often forgotten. When the generator impedance (assumed in this report to be resistive) matches the resistive component of a series-resonant load, the circuit Q becomes one-half the load Q, and the buildup to steady-state amplitude occurs in half the time interval required for a circuit having a generator of zero impedance.

Piezoelectric crystals, such as tourmaline or quartz and the polarized ceramics, usually have at least two distinct fundamental resonances: (1) a transmitting voltage response (series) resonance, and, at a higher frequency, (2) a transmitting current response (parallel) resonance. These two resonances can be understood readily by referring to either of the series circuits shown at the bottom of Fig. 18a and visualizing the existence of a capacitor C_e shunting the R_ℓ-L-C series circuit. This series-parallel combination then is the usual electrical analog of any clamped or symmetric drive piezoelectric plate where R_ℓ represents the mechanical resistance, C the compliance, and L the mass.

The capacitance C_e is that introduced by the crystal between its electroded faces, due largely to its straight capacitor action; C_e usually is referred to as the clamped capacitance.

For the frequency at which the inductive and capacitive reactances of L and C are equal, the series branch is in electrical resonance, which indicates that the crystal is in mechanical resonance.

Above this frequency, the reactance of the inductor increases until its inductive susceptance equals the susceptance of the shunting capacitor (C_e), and a parallel resonance occurs that may be described as mechanical-electrical. (This definition of parallel resonance is adequate for this report, although attention is called to the other two conditions given on page 144 of [2] that describe this type of resonance.) It is at this upper antiresonant frequency that the mechanical vibration of a quartz crystal is used to stabilize the frequency of an oscillatory electrical circuit.

The Q of the R_ℓ-L-C series branch of the circuit at resonance represents the Q_m of the piezoelectric transducer and determines the cyclic buildup time of the current pulse when the voltage applied to the circuit is constant. Constancy of driving voltage is also assumed for the usual resonance curve, with current as the ordinate. At the higher frequency where the transducer is in parallel resonance, its Q is obtained as has been described for obtaining the Q_m of the electrodynamic or magnetostrictive transducer. This is the Q of the piezoelectric transducer at antiresonance but is not Q_m, although the two may be numerically equal.

The order of occurrence of the two resonances is reversed for the electromagnetic type of transducer, whose simplified electrical analog is a parallel R_ℓ-L-C circuit in series with an inductance.

A piezoelectric sonar projector is more complex than a single crystal, with multiple resonances not always anticipated by the design engineer and variously attributed to the housing, a shift in the mode of vibration, variation in the performance of individual ceramic elements comprising an array or mosaic, or other factors.

Some experiments were made under free-field conditions to illustrate how the generator impedance influences the buildup and decay times of a pulsed signal driving a multiresonant piezoelectric projector. The oscillograms in Fig. 18b show the waveforms of high-impedance and low-impedance generators driving parallel resonant and series resonant circuits. For the moment, the discussion will include only the groups-of-three pictures labeled PROJECTOR, and will neglect the groups-of-two pictures titled CIRCUIT. Both groups are presented concurrently for ready comparison, which would be inconvenient were they placed on separate pages. Figure 18a is included to clarify the discussion of the circuits.

The groups-of-three pictures show, from top to bottom, oscillograms of driving current, driving voltage, and hydrophone output voltage associated with a resonant piezoelectric projector, as a function of the generator impedance. The two upper groups permit comparison of current, driving

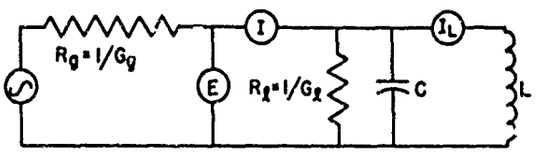

High-Z generator (constant current)
See traces 4 and 5
Q_c = Q of entire circuit
$= \omega C/(G_g + G_\ell)$
Q_ℓ = Q of load only
$= \omega C/G_\ell = I_L/I$
$Q_c = Q_\ell$ because G_g is small; E and I_L approach steady state in Q_c cps.

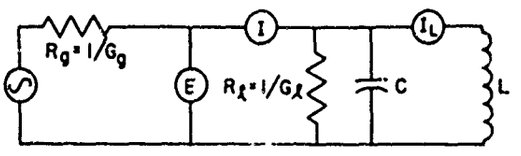

Low-Z generator (constant voltage)
See traces 9 and 10
Q_c = Q of entire circuit
$= \omega C/(G_g + G_\ell)$
Q_ℓ = Q of load only
$= \omega C/G_\ell = I_L/I$
$Q_c \neq Q_\ell$ because G_g is large; E, I, and I_L at steady state directly after transient spike.

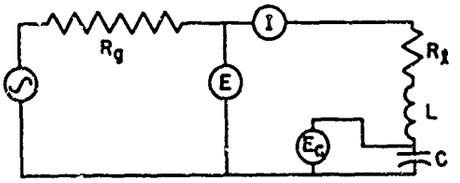

High-Z generator (constant current)
See traces 14 and 15
Q_c = Q of entire circuit
$= \omega L/(R_g + R_\ell)$
Q_ℓ = Q of load only
$= \omega L/R_\ell = E_C/E$
$Q_c \neq Q_\ell$ because R_g is large; E, I, and E_C at steady state directly after transient spike

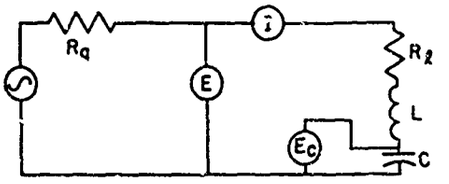

Low-Z generator (constant voltage)
See traces 19 and 20
Q_c = Q of entire circuit
$= \omega L/(R_g + R_\ell)$
Q_ℓ = Q of load only
$= \omega L/R_\ell = E_C/E$
$Q_c = Q_\ell$ because R_g is small; I and E_C approach steady state in Q_c cps.

Fig. 18a. Diagrams for electrical circuits represented by traces of Fig. 18b.

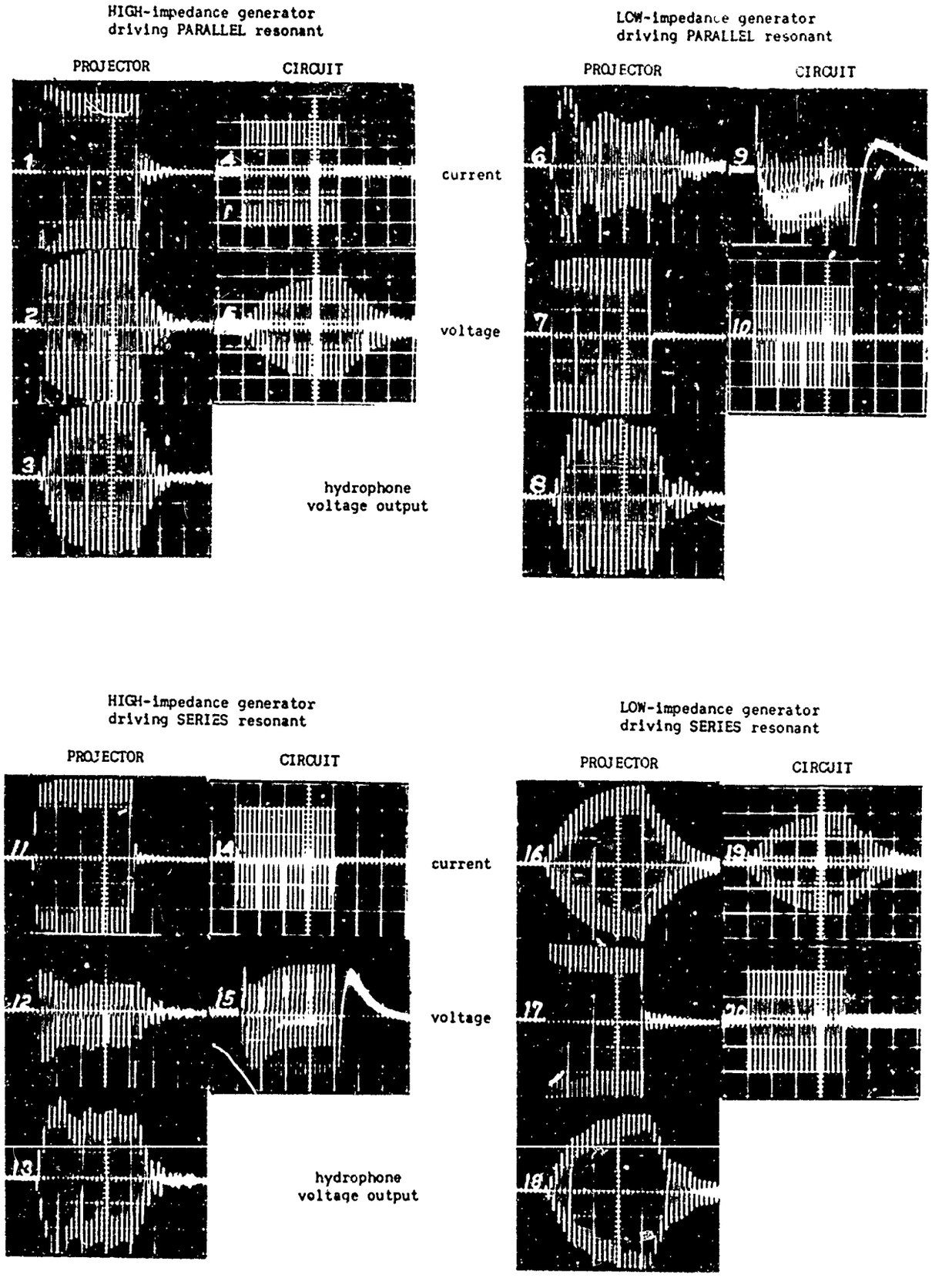

Fig. 18b. The effect of generator impedance on the buildup and decay times of a pulsed resonant piezoelectric projector at resonance frequencies of transmitting current (upper) and voltage (lower) response. Pulse shapes for similar type resonant electrical circuits are on right.

voltage, and hydrophone voltage for the case of the projector driven by high-impedance (virtually constant current)* and low-impedance (virtually constant voltage) generators at the resonant frequency of transmitting current response (TCR), or parallel resonance. The two lower groups permit a similar comparison at the frequency of transmitting voltage response (TVR), or series resonance. This particular transducer displayed a minor TVR resonance followed by a TCR resonance, and a major TVR resonance with a small increasing frequency change. That is, the response curves showed a double-hump TVR with the minor lobe at the lowest frequency, and the TCR resonant peak approximately midway between the lowest and highest frequencies. Observations made at the frequency of the minor TVR resonance showed nothing of interest, consequently photographs were made only at the two major resonances.

The transmitted pulse length in all the photographs was held at 5 msec, the equivalent of four vertical marker lines.

Trace (1) of the projector current illustrates the presence of a transient by the high initial amplitude of the pulse compared with its later steady-state amplitude. This transient indicates that the generator impedance was not large enough to drive this particular parallel-resonant circuit at constant current. If the ratio of the generator impedance to the load impedance had been greater, the current pulse would have been rectangular, and the voltage pulse of trace (2) would have approached more nearly the shape of the hydrophone output trace (3). This latter trace is shown building up to approximately 96% of steady state in 7 cycles, indicating the circuit Q = 7. This is in reasonably good agreement with Q = 8 obtained from a curve of TCR recorded from open-water measurements and computed in the customary manner. The value Q = 7 is obtained also by counting the cycles in the decay period after termination of the pulse. It should be recalled that this is not Q_m.

The buildup and decay periods will be equal only if the generator impedance when driving the load equals the generator impedance in its quiescent state when seen from the load. The impedance of the generator used in these tests happened to have the same value when measured in either direction. The effect produced at the mechanical input of the transducer by varying the load across the electrical terminals is discussed in [14]. An example of inequality of generator impedance is that of a cathode-follower type of driver.

The group-of-three pictures at the upper right in Fig. 18b may be compared directly with those to the left, the only change being the substitution of a low-impedance generator. The conductance of the generator is now high and is no longer negligible. It lowers the circuit Q to approximately 4. Traces (6) and (8) show what appears to be modulation

*When the generator impedance is infinitely high, the generator is described as a constant-current one. In a constant-current source, the generated voltage is infinite and the internal resistance is also infinite, but the ratio of generated voltage to internal resistance is finite and equal to the current supplied [16].

by a lower frequency. The wavelength of this undulation made it appear to be the result of a beat frequency between the TCR resonant frequency and the frequency of TVR resonance.

The hydrophone output trace (18) shows that a 15-cycle buildup time is required to approximate the steady-state condition, giving a mechanical Q = 15. This is in good agreement with $Q_m = 16$ computed as previously described from a plotted curve of the TVR of the projector. In this case the low impedance of the generator makes R_g negligible, and again only the Q of the load is measured. A comparison of the hydrophone output traces (13) and (18) illustrates the decrease in buildup time when R_g becomes appreciable and the circuit Q is lowered to approximately 3.

The wavelength of the ripple impressed on the voltage and hydrophone output traces (12) and (13) was at first assumed to be the same as that shown by the current and hydrophone output traces (6) and (8). However, a closer study showed that this beat frequency was considerably higher. Electrical interference was suspected, and additional photographs were made of the hydrophone output trace, with longer pulse lengths to determine when, if ever, steady-state condition was attained. When the pulse duration was quadrupled to 20 msec, steady-state condition was finally obtained. The ripple almost completely disappeared after 15 msec. Calculation indicated another higher resonant frequency with Q = 60 that apparently had gone unnoticed. Re-examination of the original calibration recorder traces proved that this hypothesis was correct. For all practical purposes, this ripple would have had little influence on measurement accuracy. From an academic viewpoint, however, it was interesting that Q number of cycles at the driving frequency may be entirely unrelated to the interval needed by the pulse to reach steady-state condition.

GENERATOR IMPEDANCE AND Q

The same lack of understanding mentioned in the section "Transducer Q" has been observed concerning the Q associated with simple parallel and series circuits under pulsed excitation. Use of the following indefinite statements, which may be true or false, is common:

(1) The voltage across the reactance of a series-resonant circuit is Q times the applied voltage; or, the current circulating through the reactances of a parallel-resonant circuit is Q times the generator current.

(2) A pulse builds up to 96% of steady-state magnitude in Q number of cycles in either a parallel or a series resonant circuit.

This confusion disappears when it is recognized that the Q of statement (2) differs in magnitude from the Q of statement (1) except for a single theoretical condition that can be approached, but not attained, experimentally. The Q's are identical only when the series resonant circuit is driven with constant voltage or the parallel resonant circuit is driven at constant current. When these two Q's are defined and identified by appropriate subscripts, all ambiguity disappears.

The Q referred to in statement (1) is the Q of the load only (Q_ℓ). The Q of statement (2) is the Q of the entire circuit (Q_c).

In the electrical series-resonant circuit,

$$Q_\ell = \frac{X_L}{R_\ell} \qquad \text{and} \qquad Q_c = \frac{X_L}{R_\ell + R_g} \qquad \text{where}$$

Q_ℓ = Load Q

Q_c = Circuit Q

X_L = Reactance of the load inductance (ωL)

R_ℓ = Resistance of the load

R_g = Resistance of the generator

In the electrical parallel-resonant circuit,

$$Q_\ell = \frac{B_\ell}{G_\ell} \qquad \text{and} \qquad Q_c = \frac{B_\ell}{G_\ell + G_g} \qquad \text{where}$$

Q_ℓ = Load Q

Q_c = Circuit Q

B_ℓ = Susceptance of the load capacitance (ωC)

G_ℓ = Conductance of the load

G_g = Conductance of the generator ($1/R_g$)

The groups-of-two pictures of Fig. 18b show the similarity of current and voltage pulse shapes for resonant electrical parallel and series circuits. No attempt was made to make the circuits equivalent to the projector; a 5-mH inductor was connected in series or in parallel with a 235-nF capacitor, and the circuit was driven with pulses of 4 msec duration at approximately 5 kc.

Note the similarity in the distortion of the current pulse in trace (9) and the voltage pulse of (15). The fundamental frequency is nearly absent from both traces and the harmonic content is accentuated because of the increased amplifier gain necessary to obtain uniformity of amplitude in the photographs. The error in measuring the absolute amplitude

of either of these pulses with a wideband amplifier is obvious, and demonstrates an additional handicap inherent in pulse-testing practice. The same distorted sinusoids in the pulse would be evident in c-w testing except for the general use of narrow-band filters.

The harmonic frequencies in the current pulse of trace (9) are predominant when a constant-voltage generator is used because they are at a lower impedance level than the fundamental when the load circuit is antiresonant. This is a high-Q current circuit with complete absence of voltage resonance. To obtain the high-Q voltage resonance, a constant-current generator must be used, as illustrated in trace (4).

Similar reasoning may be applied to the voltage trace (15) of the series-resonant circuit driven by a high-impedance generator. A series-resonant load circuit presents minimal resistance to the generator at the resonant frequency. When the generator resistance is high, the load is virtually a short circuit at the frequency of resonance; consequently, the voltage across the load is very low. At frequencies off resonance, the impedance of the load increases, and harmonic voltages may be measured.

These oscilloscope traces may be understood more easily by reference to their related schematic diagrams in Fig. 18a. The driving impedances used in ordinary measurement practice will vary, of course, between the limits of constant voltage and constant current that are shown.

PULSED MEASUREMENTS OF REFLECTION AND ABSORPTION

This report would be incomplete without some mention of the use of pulsed sound to measure the transmission, reflection, and absorption of plates. The Navy requires that large reflecting baffles operate at high hydrostatic pressure for sonar targets or sound screens; at great depths in the ocean, these may become transparent. Research has been continuous in this specialized field to find underwater sound absorbers or reflectors whose characteristics would be unaffected either by temperature or pressure. These materials must be evaluated in a closed tank so that temperature and pressure can be controlled; thus, small samples must be used. These tests require the use of pulsed sound, not only to eliminate reflections, but also to avoid diffraction effects created by the finite size of the plate.

The method of measurement was first described by W. J. Trott and the writer in an oral paper, "The Measurement of the Acoustic Properties of Sound-Absorbent Panels at High Hydrostatic Pressures" presented at the 39th meeting of the Acoustical Society of America in 1950. The paper was not published at that time. Three years later the measurement technique was described briefly [17] excluding both the theory of pulse modulation and of the near-field (Fresnel region) of a square plate. The latter theory is now available as [18]. The method described by Trott and Darner remains virtually unchanged. Any refinements may be attributed to use of a larger pressure vessel, improved probe hydrophones, increased size of plates, and temperature control.

A brief review of a decade-old method will serve as an introduction to a technique of absorption measurements that was developed almost entirely on an empirical basis. An omnidirectional probe hydrophone was positioned in front of a square steel plate on an imaginary line joining the centers of the plate and of a distant projector, the faces of both being normal to the line. The pressure of a short pulse of sound from the projector was measured as it passed the probe on its way to the plate. The pulse pressure was measured again after reflection from the plate and before receipt of diffracted sound contributions from the edges of the plate. Because of the greater distance of travel and the proximity of the sound source, the reflected sound amplitude had to be corrected according to the inverse square law distance loss. The ratio of the measured amplitudes of the distance-corrected reflected sound energy and the incident energy was a measure of the plate reflectivity.

The measurement of sound transmission through the plate was even simpler; the magnitude of the sound received by the probe without the plate in position was compared with that received before the diffracted sound when the plate was inserted ahead of the probe to shadow it from the projector. The pulse technique, of course, permitted the measurement to be made before the energy diffracted by the plate arrived at the receiver. The sum of the reflected and transmitted sound energies (not pressures) should have been very nearly 100%, provided that there was no measurable absorption in the steel plate. Sound-absorbing materials were then glued to the face of this plate and their measured lack of reflectivity (with zero transmission) was termed absorption.

The initial reflection and transmission measurements are always made with a bare steel plate to check:

(1) Perpendicularity of plate to sound beam

(2) Equality of response of probe hydrophone faces

(3) True inverse-square distance loss

(4) Ability of the system operator to eliminate sound diffracted by the plate edges by adjusting the receive gate.

From the foregoing description, one might conclude that these measurements can be made without difficulty. Just the opposite is true, for they are undoubtedly the most difficult to make of any of the types of measurements in the anechoic tank.

An understanding of the theory associated with these measurements helps in acquiring valid data. The 5/8-inch thickness for the reflecting plate was chosen many years ago. At that time, requested measurements were in the frequency range 10 to 150 kc and the thickness of the plate was calculated for its maximal reflectivity over that range.

The equation given by Rayleigh [19] nearly 100 years ago for the sound energy reflected from a plate is of the form:

$$R = \frac{\left(\frac{\rho c}{\rho_1 c_1} - \frac{\rho_1 c_1}{\rho c}\right)^2}{4 \cot^2 \frac{2\pi L}{\lambda_1} + \left(\frac{\rho c}{\rho_1 c_1} + \frac{\rho_1 c_1}{\rho c}\right)^2}$$

where R = reflected energy, ρ = density of medium, ρ_1 = density of plate, c = sound velocity in medium, c_1 = sound velocity in plate, L = thickness of plate, and λ_1 = wavelength of sound in plate.

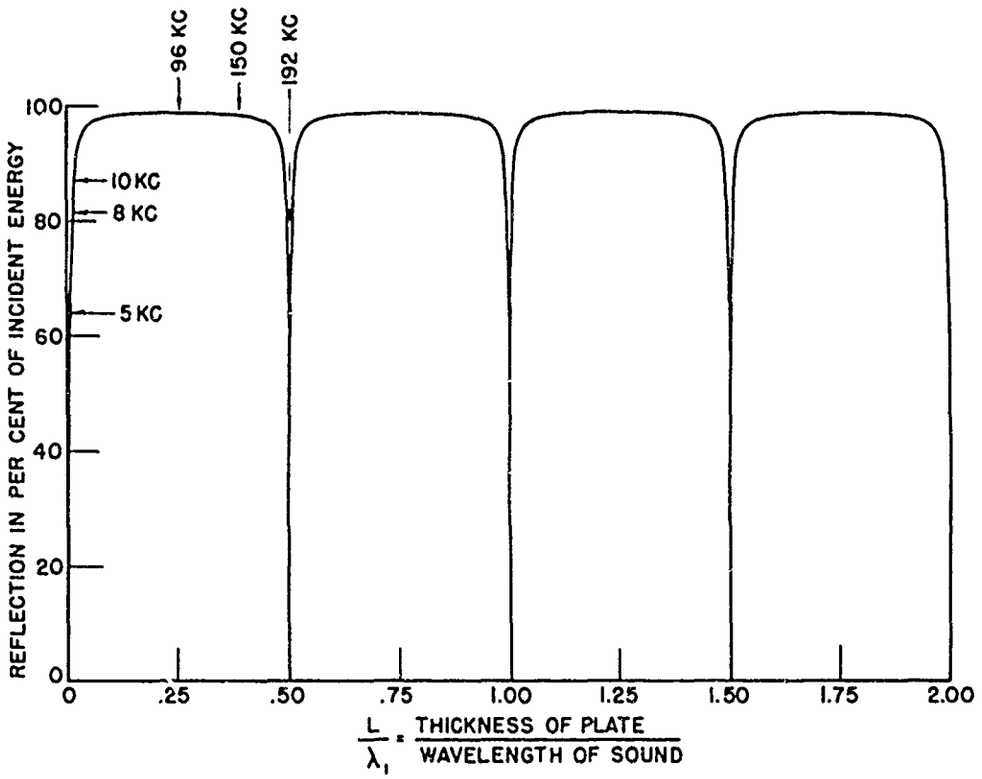

Fig. 19. Sound energy reflected from steel plate. Frequency values are for plate of 5/8-inch thickness.

The calculated reflectivity of any steel plate is shown in Fig. 19 as a function of the ratio of its thickness to the wavelength of sound in the material. Note that the plate is an almost perfect reflector when the thickness is an odd multiple of quarter wavelengths, with total transmission occurring at the even multiples. The frequencies indicated on the curve between 0 and 0.50 on the abscissa apply for the standard 5/8-inch plate. In recent years there has been a consistent trend toward lower and lower frequencies. At frequencies below 5 kc, the 5/8-inch plate transmits considerable energy. The use of a thicker plate has been considered, but the gain in reflectivity is more than offset by the increased rigging problems associated with a heavy plate. The substitution of a

1-inch plate for the one now in use would increase the energy reflected at 5 kc approximately one dB, or to the point marked "8 kc" on the curve. A 2-inch-thick plate would be required to approach total reflection at 5 kc, and its weight would be a rather unwieldy quarter of a ton.

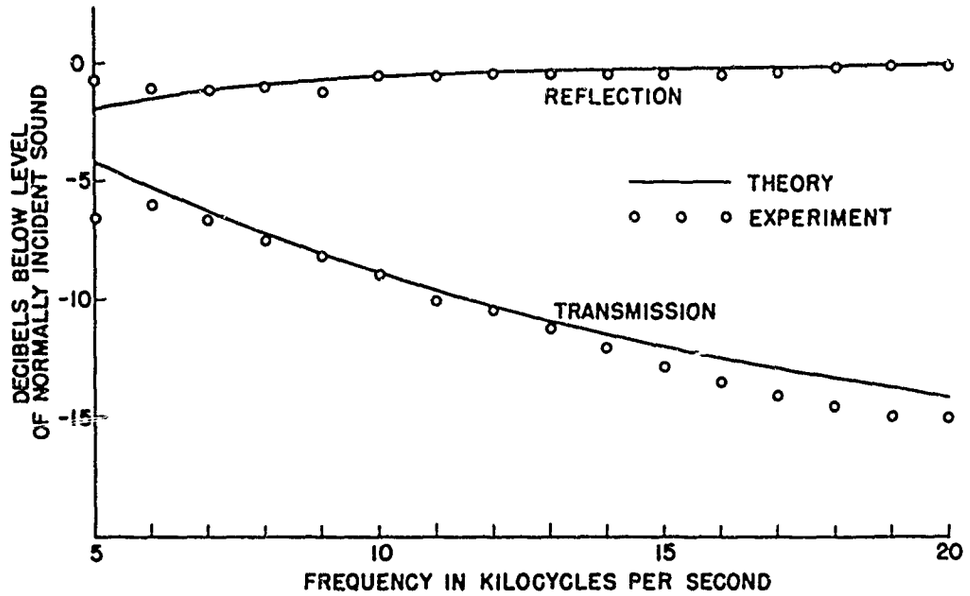

Fig. 20. Theoretical reflection and transmission compared with experimental results for a 5/8-inch stainless steel plate.

The measured sound reflection and transmission for a stainless steel plate of 5/8 inch thickness are compared in Fig. 20 with Rayleigh's theoretical curves. Data at frequencies above 20 kc have been omitted because the sound energy is almost totally reflected as the plate thickness approaches a quarter wavelength. Note that the excess of measured reflected energy over that predicted by theory at 5 and 6 kc is compensated by the low value for transmitted energy. At 6 kc the sum of the two measured energies gives a total that is only 4% too high.

Unlike the thickness of the plate, the requirements for which can be determined mathematically, the side dimensions are limited by the diameter of the porthole through which the plate must be rigged. When the measurement of diffraction contributions is to be avoided this limitation of the plate width to 30 inches determines the lower limit of the test frequency.

The theory developed for an underwater sound projector or a radar antenna can be applied to the near field (Fresnel diffraction region) of a reflecting plate. The radar antenna presentation was chosen from [20] because of its relative clarity and mathematical simplicity, and because the effects of square and circular configurations can be compared.

The on-axis power densities of uniform square and circular apertures are plotted in Fig. 21. A coefficient has been chosen to normalize the power density or sound intensity to one at $R = 2L^2/\lambda$, where R = distance from probe hydrophone to plate, L = length of side of square, and λ = wavelength in water = speed/frequency. The similarity of the diffraction effects about apertures, plates, and projectors permits use of these three terms interchangeably.

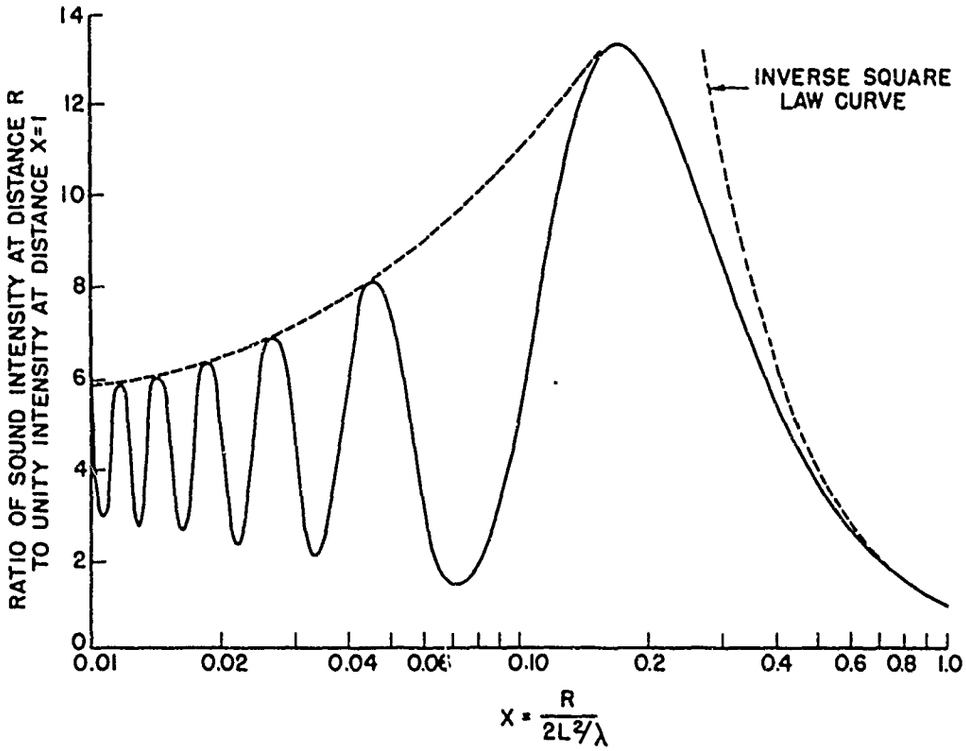

Fig. 21a. On-axis power density, uniform square aperture.

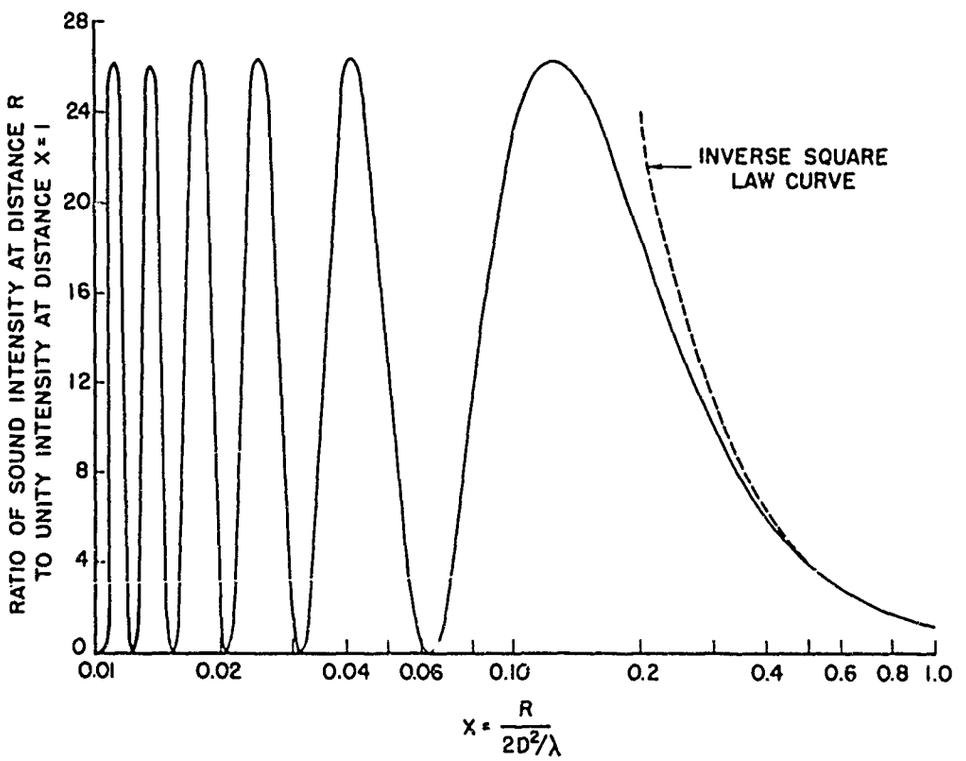

Fig. 21b. On-axis power density, uniform circular aperture.

Use of these curves makes possible approximate solutions without the mathematical tedium associated with point-by-point calculations using Fresnel integrals, which are described in [21] and tabulated in its third appendix.

Some additional explanation may save the novice considerable time in the use of these curves, which are important in visualizing the transition of the sound field along the axis connecting the near field (Fresnel diffraction) and the far field (Fraunhofer diffraction). It is in this intervening region that most of the acoustic evaluation measurements take place. The divergence of sound intensity from the near-perfect inverse-square law gain with decreasing distance to the reflecting plate or projector is readily seen. Diffraction phenomena as shown by the figures should be understood and their unwanted appearance recognized and avoided in pulsed acoustic reflection measurements.

Only the square aperture is discussed here because an understanding of the circular aperture readily follows. The only difference in the two formulae lies in the substitution of the diameter D of the circle for the side L of the square.

The ordinates of Fig. 21 compare the undulating intensity near the face of the plate with the reference level 1 measured at a distant point. The distance of this point from the plate is represented by the abscissa value 1.0 at the extreme right; that is, $X = 1$ when the probe hydrophone distance $R = 2L^2/\lambda$.

Because only frequency is varied during measurements of plate reflection, the formula may be changed into the more convenient form $X = Rc/2L^2f$ by substituting sound speed c and frequency f for the wavelength λ. In this form, X is an inverse function of frequency because R, L, and c remain constant during any particular series of measurements. That is, as frequency increases, the position of the measuring probe appears to approach the plate and possibly shift from the far field to the near field.

At the distance $X = 1.0$, spherical-wave divergence is shown by a comparison of the intensity at this point with that shown by the curve at $X = 0.707$. The intensity varies as the square of the ratio of the distances: $(1/0.707)^2 = (1.414)^2 = 2$, which is in agreement with the intersection of the curve and the ordinate. These two distances may be regarded as being in the far field with accompanying Fraunhofer diffraction.

By a further decrease of test distance to $X = 0.5$, a transition zone appears that connects the near and far fields. The square of the distance ratio should again double the intensity: $(0.707/0.5)^2 = (1.414)^2 = 2$. The curve fails to reach this level, however, and measurements taken in this region are subject to this error. The error becomes intolerable with decreasing measurement distance.

A comparison of the upper and lower charts shows that, for equal error, measurements can be made nearer to a circular plate or projector than to a square. For the circular configuration, the proper distance loss is still evident on the curve at $X = 0.5$ ($R = D^2/\lambda$), that is, $(1/0.5)^2 = 4$. From this observation, the conclusion may be drawn that the square shape should be tested at 1.4 (ratio of diagonal to side) times the distance used for the circular shape. A technical discussion of near and far fields for the circular shape only appears on pages 59-72 of [8].

When test frequency is the variable, the formula for the curve of Fig. 21a is:

$f = (Rc/2L^2X)$, where

f = frequency of a maximum or a minimum

R = distance from probe hydrophone to plate
(the distance 39.5 cm was chosen for the data of Fig. 22)

c = speed of sound (1.5×10^5 cm/sec)

L = length of side of square (30 in = 76 cm)

X = numerical value of abscissa where max or min occurs

Insertion of the parameters for the specific conditions of the test simplifies the formula to:

$f = (0.51/X)$ kc.

When X is given the successive values 0.032, 0.045, and 0.070, the curve predicts a minimum at 16 kc, a maximum at 11.3 kc, and a minimum at 7.3 kc, respectively. The agreement in frequency between theory and experiment is shown by the solid curves of Fig. 22. These two curves were recorded with slightly different pulse lengths and show the magnitude of measurement error that can occur because of diffraction contributions from the plate edges. Without some understanding of the theory, the apparent lack of reflection at the minima of the curves could be misinterpreted as the result of absorption. The dashed curve was made with a properly reduced pulse length to avoid the edge effects and to make the size of the plate appear infinite to the probe. Even with the probe distance reduced to 30 cm, the received pulse must be shorter than 0.2 msec, which necessitates the recording of less than one cycle at the minimal test frequency 5 kc.

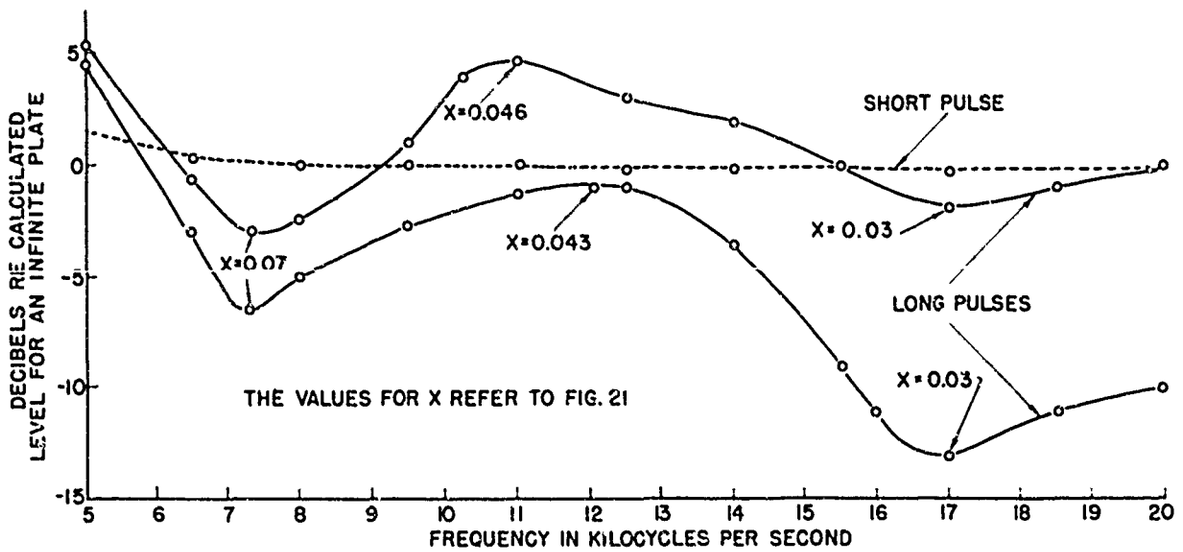

Fig. 22. Measured reflection from steel plate; the values of X refer to Fig. 21.

When the sound-absorbing coating on the test plate is of the resonant type, the technique required for its evaluation differs from the method usually employed on nonresonant materials. A resonant absorber may be defined as one having high echo-reduction over a very narrow frequency band. Supposedly, it would possess a mechanical Q equal to the frequency of minimal reflection divided by the difference in the frequencies at the levels 3 dB higher.

The theory of the resonant sound absorber is developed briefly in [22] and will not be repeated in this report, which deals with the evaluation of the material by pulsing methods rather than its development and construction. Reference [22] mentions that the resonant absorber is analogous to an electrical parallel resonant circuit in which the a-c potential corresponds to a mechanical alternating force, and the a-c current to the velocity amplitudes of the absorber elements. This analogy is acceptable for this report, although some writers prefer other theories. Usually, the acoustic impedance of the absorbing material is assumed to be matched to that of water.

As with its electrical counterpart, a mechanical resonant circuit ordinarily requires Q number of cycles to approach within 4% of the steady-state condition. A resonant circuit having Q = 10 with a water load should not be measured with a pulse of less than ten cycles if reasonable accuracy is to be attained. Pursuing this line of reasoning, the lower test frequency for a resonant absorber 76 cm square with Q = 10 would be limited to 67 kc for a received pulse length of 150 μsec measured acoustically at the very beginning of the pulse. Or, measurement at the frequency 5 kc would require a pulse length of 2 msec, which is ten times the length permissible for the avoidance of the edge diffraction effects.

A reflection measurement made prior to Q number of cycles must be regarded as qualitative rather than quantitative. There is no way to avoid the fact that a number of cycles equal to the Q of the mechanical vibrating system is necessary to obtain a correct measure of the echo reduction.

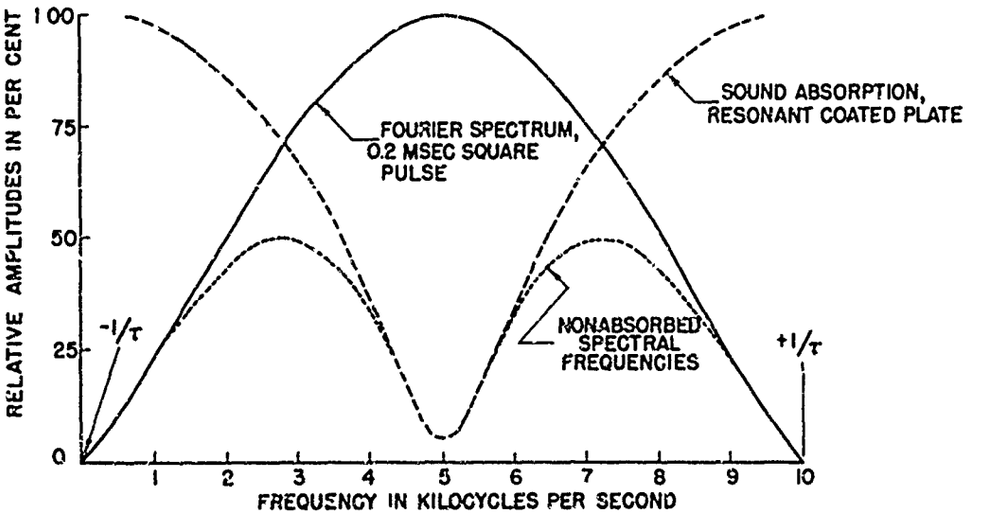

Fig. 23. Residual spectral frequencies of short pulse reflected from a resonant absorber.

A hypothetical example of a resonant absorbing system with Q = 10 is plotted as the dashed curve in Fig. 23. At its resonance frequency 5 kc, the pressure reflectivity is 5%, or 26 dB lower than that of a perfect reflector. This point of minimal reflectivity is to be measured with a square pulse envelope having a duration of 0.2 msec. The Fourier spectrum of its main lobe only is plotted as the solid curve centered at the frequency of interest.

Note that most of the absorption occurs in a 3-kc band centered at 5 kc; the spectral frequencies below 3.5 kc and above 6.5 kc receive negligible attenuation. The amplitudes of the spectral frequencies that were only partially absorbed are enclosed by the dotted curve, which is the product of the per cent pressure reflected and the original relative amplitudes at each spectral frequency. When the square pulse is reconstructed by summation of the spectral frequency amplitudes, the measured level of the envelope is found to have been decreased by only 6 dB rather than the 26 dB that is shown.

The foregoing also may be regarded as a graphical representation of a pulsed signal unable to follow into a narrow, deep null in transducer response measurements where the sideband amplitude is increasing in two directions.

This error in measurement can be reduced considerably by using the repeated pulse excitation of a narrow band filter that has been described under "Technique for Measurement of Spectrum." Measurements on one particular resonant sample, using this method, showed the reflected sound energy reduced 99½%. This was in considerable contrast to the usual method, which showed far higher reflectivity. Admittedly, the higher measurement of absorbed energy was inexact, but it at least provided some evaluation of the possibilities of the material whose exact worth could not be determined by any other method.

During wideband measurements of this particular resonant absorber, photographs were made of the reflected pulse appearing on the oscilloscope. A study of these pictures showed the nearly complete absence of the fundamental frequency during excitation of the sample. When the pulse terminated, however, the fundamental frequency appeared as a highly-damped signal with the initial cycle of magnitude sufficient to indicate total reflection. This anomalous trailing transient was thought to be either the product of plate-edge diffraction or the oscillatory decay of the mechanical vibrating system. Diffraction from the edges did not seem plausible because the high sound absorption connoted an acoustical impedance matching that of the water; then the plate edges, presumably, would not act as a boundary.

The alternate theory (oscillatory decay of the mechanical vibrating system) seems reasonable when the resonant absorber is considered to change from a nonreflector of incident sound to a radiator of its stored sound energy upon cessation of the pulse. The junction of the pulse termination and its transient might be explained as a discontinuity in the oscillatory phase of the reflected pressure wave. An attempt has

been made in Fig. 24 to illustrate the probable mechanical displacement of the plate. Both the figure and the following explanation are entirely hypothetical.

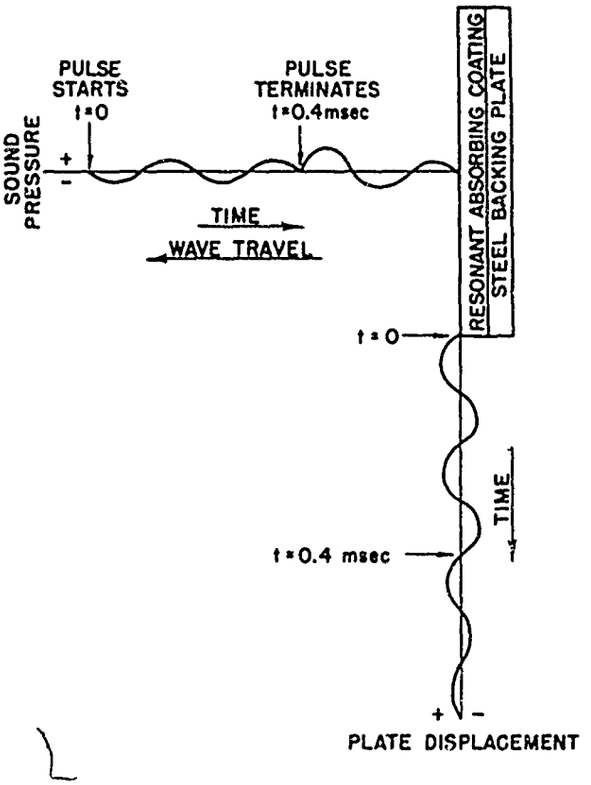

Fig. 24. Phase reversal in reflection from resonant absorber at termination of pulse.

The assumed frequency 5 kc permits the presentation of a two-cycle pulse from t = 0 to t = 0.4 msec. Even though the final half-cycle of the reflected pulse is a compression, it is followed immediately by another compression rather than the rarefaction usually encountered in sinusoidal vibration. This occurs because the sound wave reflection is 180° out of phase with the plate motion. When the material is absorbing, positive sound pressure causes negative plate displacement; but when the material is radiating, negative displacement causes negative pressure. When the pulse is terminated, the final half-cycle of the reflected pulse is headed toward negative pressure while the plate travels toward a positive displacement to create the second compressional wave. This follows Newton's First Law of conservation of momentum.

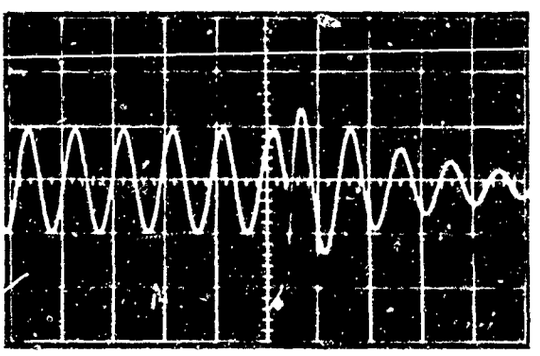

Fig. 25. Phase reversal of the transient current in a parallel-resonant electrical circuit upon termination of the pulse.

The same effect appears in the current waveform of the analogous parallel-resonant electrical circuit. This effect for Q = 8 is shown in Fig. 25 to the right of the center line, where the current waveform

reverses its direction at the abscissa when the pulse terminates. Similar reversal of the voltage waveform occurs in a series-resonant circuit.

ACKNOWLEDGMENTS

The author wishes to thank Mr. R. J. Bobber and Mr. W. J. Trott for their sound reviews, constructive criticisms, and many helpful discussions.

REFERENCES

[1] S. Goldman, Frequency Analysis, Modulation and Noise (McGraw-Hill Book Company, Inc., New York, 1948), pp. 30-32.
[2] F. E. Terman, Radio Engineers Handbook (McGraw-Hill Book Company, Inc., New York, 1943), p. 22.
[3] C. Cherry, Pulses and Transients in Communication Circuits (Dover Publications, Inc., New York, 1950).
[4] W. L. Sullivan, "Analysis of Systems with Known Transmission Frequency Characteristics by Fourier Integrals," Electrical Engineering, Vol. 61, No. 5, May 1942.
[5] "American Standard Procedures for Calibration of Electroacoustic Transducers, Particularly Those for Use in Water, Z24.24-1957."
[6] M.I.T., Principles of Radar (McGraw-Hill Book Company, Inc., New York, 1946), pp. 4-22.
[7] R. J. Bobber, "Dimensions of Test Tanks for Underwater Transducer Measurements," USRL Research Report No. 39, 23 Aug 1956.
[8] T. F. Hueter and R. H. Bolt, Sonics (John Wiley and Sons, Inc., New York, 1955), p. 383.
[9] K. Henney, Radio Engineering Handbook (McGraw-Hill Book Company, Inc., New York, 1941), p. 38.
[10] W. J. Remillard, J. Acoust. Soc. Am. 31, 531-534 (1959).
[11] Summary Technical Report of NDRC Division 6, Vol. 12 (1946), pp. 173-177.
[12] F. V. Hunt, Electroacoustics (John Wiley and Sons, Inc., New York, 1954), pp. 98-99.
[13] P. Vigoureux, Ultrasonics (John Wiley and Sons, Inc., New York, 1951), p. 10.
[14] C. L. Darner and R. J. Bobber, J. Acoust. Soc. Am. 27, 908-912 (1955).
[15] R. M. Kerchner and C. F. Corcoran, Alternating Current Circuits (John Wiley and Sons, Inc., New York, 1946), 2nd ed., pp. 502-531.
[16] W. L. Everitt, Communication Engineering (McGraw-Hill Book Company, Inc., New York, 1937), pp. 65-66.
[17] C. L. Darner, USRL Research Report No. 31 (U. S. Navy Underwater Sound Reference Laboratory, 1953), App. 1.
[18] H. Stenzel, "Die akustische Strahlung der rechteckigen Kolbenmembran (The Acoustic Radiation of a Vibrating Rectangular Rigid Membrane)," Acustica 2, 263-281 (1952).
[19] J. W. S. Rayleigh, The Theory of Sound, Vol. 2 (Dover Publications, New York, 1945), p. 88.
[20] R. W. Bickmore and R. C. Hansen, Proc. IRE 47, 2119 (1959).
[21] R. H. Randall, An Introduction to Acoustics (Addison-Wesley Press, Inc., Cambridge, Mass., 1951), pp. 89-93.
[22] E. G. Richardson, Technical Aspects of Sound, Vol. 2 (Elsevier Publishing Company, New York, 1957), pp. 287-327.